

Application Grade Thesis

Title:

Scaffolding techniques and tissue imaging on them

Τεχνικές Κατασκευής Ικριωμάτων και απεικόνιση ιστού σε αυτά

Student's Name: Daskalakis Panagiotis

Supervisor's Name: Dr. Stratakis Emmanuel

Date of completion: March 2022

This dissertation is submitted as a partial fulfilment of the requirements for the Master's degree of Biomedical Engineering M.Sc. program

Acknowledgements

The physical models and results that are presented in this thesis were conducted and produced in Stratakis Lab – ULMNP – IESL FORTH. Materials and further expenses were all provided by Dr. Stratakis.

I am grateful to my professor, mentor, and colleague Dr. Emmanuel Stratakis for introducing me to Tissue engineering through his lectures, and for providing me with a great working environment, high-end technology, and educational support for my scientific future.

Special thanks to my LaBio group (Dr. Paraskevi Kavatzikidou, Dr. Lina Papadimitriou, Dr. Anthi Ranella, Dr. Eleftheria Babaliari, Dr. Phanee Mangana, Ms. Eleni Kanakousaki, Ms. Lefki Chaniotaki, and Mr. Alkaios Lamprakis) not only for their co-operation and assistance, but for helping me realize how wonderful is the world of material science, biology, engineering, and medicine.

To Christos Ntoulas, I am grateful for having a colleague and a friend like you, spending days designing and troubleshooting for something new for both of us, but always finding a way to solve it.

This research is dedicated to my parents who motivate, protect, and encourage me to chase my dreams.

Abstract

Regenerative medicine and tissue engineering have recently been a trending scientific field in the world of modern medicine. The future of tissue engineering is highly promising offering solutions for successful transplantation, repair, regeneration, and self-healing of tissue, organoids, and organs. 3D printing is a promising technique used as a fabrication methods in creating scaffolds for tissue engineering. Great advantages using the 3D printing technique are proved to be in creating complex geometries, gradient porosities, and co-culture of numerous cells, using well-developed biomaterials. Thus, these applications are limited caused of the low variety in biomaterials and construction mechanisms that are used yet.

The purpose of this thesis research is the conversion of a standardized 3D printer to an ultra-low-cost 3D-4D bioprinter (constructed from PLA 3D printed parts), and the construction of 3D-4D scaffolds for cellular responses such as adhesion and proliferation. Cellulose acetate is the chosen bioink for the bioprinted structure because of the flexible printability of the mixture and the high mechanical properties, Cellulose Acetate offers. Parametric calculations for the extrusion manipulation are presented in boards, and firmware commands that had to be changed for temperature safety factors (fluid and not fused material) are presented as well. 3D scaffolds were designed and developed into Gcode files for the bioprinter to fabricate, delivering high-quality bioprinted scaffolds after modification of the printing parameters, bioprinting-mechanism, and bioink composition. The results showed that the CA scaffolds created from the converted bioprinter offered a better geometrical structure and resolution compared to other printed scaffolds. Future research is focused on the development of advanced bioinks, more accurate geometrical modeling, and in-vitro cytocompatibility studies.

Περίληψη

Η αναγεννητική ιατρική και η μηχανική ιστών είναι πρόσφατα ένα δημοφιλές επιστημονικό πεδίο στον κόσμο της σύγχρονης ιατρικής. Το μέλλον της μηχανικής ιστών είναι πολλά υποσχόμενο, προσφέροντας λύσεις για επιτυχή μεταμόσχευση, επισκευή, αναγέννηση και αυτοθεραπεία ιστών, οργανοειδών και οργάνων. Η τρισδιάστατη εκτύπωση είναι μια πολλά υποσχόμενη τεχνική που χρησιμοποιείται ως μέθοδος κατασκευής στη δημιουργία κριωμάτων για τη μηχανική ιστών. Μεγάλα πλεονεκτήματα με τη χρήση της τεχνικής τρισδιάστατης εκτύπωσης αποδεικνύεται ότι είναι στη δημιουργία πολύπλοκων γεωμετριών, βαθμωτών πορώδων και συν-καλλιέργειας πολυάριθμων κυττάρων, χρησιμοποιώντας καλά ανεπτυγμένα βιοϋλικά. Έτσι, αυτές οι εφαρμογές είναι περιορισμένες λόγω της χαμηλής ποικιλίας σε βιοϋλικά και κατασκευαστικούς μηχανισμούς που χρησιμοποιούνται ακόμη.

Σκοπός της παρούσας διατριβής είναι η μετατροπή ενός τυποποιημένου τρισδιάστατου εκτυπωτή σε έναν εξαιρετικά χαμηλού κόστους βιοεκτυπωτή 3D-4D (κατασκευασμένος από εκτυπωμένα μέρη PLA 3D) και η κατασκευή κριωμάτων 3D-4D για κυτταρικές αποκρίσεις όπως η πρόσφυση και ο πολλαπλασιασμός. Η οξική κυτταρίνη είναι το επιλεγμένο βιομελάνι για τη βιοεκτυπωμένη δομή λόγω της ευέλικτης δυνατότητας εκτύπωσης του μείγματος και των υψηλών μηχανικών ιδιοτήτων, που προσφέρει. Οι παραμετρικοί υπολογισμοί για τον χειρισμό της εξώθησης παρουσιάζονται σε πίνακες και παρουσιάζονται επίσης εντολές υλικολογισμικού που έπρεπε να αλλάξουν για τους παράγοντες ασφάλειας θερμοκρασίας (ρευστό και όχι συντηγμένο υλικό). Τα τρισδιάστατα κριώματα σχεδιάστηκαν και αναπτύχθηκαν σε αρχεία Gcode για την κατασκευή του βιοεκτυπωτή, παρέχοντας βιοεκτυπωμένα κριώματα υψηλής ποιότητας μετά από τροποποίηση των παραμέτρων εκτύπωσης, του μηχανισμού βιοεκτύπωσης και της σύνθεσης του βιοεκτυπώματος. Τα αποτελέσματα έδειξαν ότι τα κριώματα CA που δημιουργήθηκαν από τον μετατρεπόμενο βιοεκτυπωτή πρόσφεραν καλύτερη γεωμετρική δομή και ανάλυση σε σύγκριση με άλλα τυπωμένα κριώματα. Η μελλοντική έρευνα επικεντρώνεται στην ανάπτυξη προηγμένων βιομελανών, ακριβέστερης γεωμετρικής μοντελοποίησης και in vitro μελετών κυτταροσυμβατότητας.

Table of contents

Table of Contents

Acknowledgements	2
Abstract.....	3
Table of contents	5
List of figures.....	7
List of tables.....	9
Chapter 1: Introduction	10
Regenerative medicine	10
Tissue engineering	10
Tissue engineering: Biomaterials	11
Tissue engineering: Cells.....	11
Tissue engineering: 2D – 3D – 4D bioprinting.....	11
Scaffolds in medicine	12
Biofabrication	12
Fused Deposition Modeling	12
Computer-aided design	13
Thermoplastic materials	14
3D – 4D Bioprinting.....	14
Biomaterials	14
3D – 4D Scaffolding.....	14
Chapter 2: State-of-the-art	15
.....	22
Chapter 3: Research methodology	23
Chapter 4: Research findings / results	24
Designing the bioprinting head.....	24
Mechanism functionality calculations	25
3D modeling of the bioprinting head.....	27
Presenting the 3D modeled parts	28
Printing procedure of the parts	33
Final assembly of parts	34
Converting the mechanism into an automatism	35
Preparation of the bioink.....	36

First printing result	37
Preliminary Cell Study on CA scaffolds	38
Scanning electron microscopy (SEM): preparation of the biological samples - dehydration procedure	38
Chapter 5: Discussion and analysis of findings	39
Optimization process for the successful Cellulose Acetate printing.....	39
Comparing the results with literature's	41
Biocompatibility – Toxicity tests	43
Comparing structure architecture with efficiency	44
Chapter 6: Conclusion and recommendations	46
References	47

List of figures

Figure 1: Circle of tissue engineering by (Asadian, 2020)	10
Figure 2: Bioinks referred to the Cell type/Tissue that they can regenerate.....	11
Figure 3: Illustrative diagram representing the addition of a predesigned stimulus to promote a desired change at the construct. (Morouço, et al., 2020)	11
Figure 4: Standard view of a designed 3D model. Blue lines indicate the 2D sketch design and then by command extrude the 2D bulks into 3D (Illustration by author).....	13
Figure 5: A) 3D-printed temporal bone model following dissection for pre-operative surgical simulation. (B) Intraoperative photo for comparison status post-CWD tympanomastoidectomy, demonstrating the horizontal semi-circular canal (HSSC), the sigmoid sinus (SS) and facial nerve (FN) (Rose, et al., 2015)	15
Figure 6: Tissues vary in their structure, function, and origin. (Simply science, n.d.).....	16
Figure 7: Print fidelity of the ink showing (A) printing of grid-like structure (i) extrusion of the ink through the nozzle, (ii) initial few layers, and (iii) formed grid-like pattern; (B) fabrication of human anatomical ear (i) CAD model and generated STL file, (ii) generated Gcode using slicer, (iii) printing process, and (iv) printed ear structure	17
Figure 8: Extrusion mechanisms based on the requirements of the bioink (Zeming Gu, 2020).....	18
Figure 9: 3D bioprinting of skin tissue: Provided by (Askari, et al., 2020)	18
Figure 10: Folding mechanism of the gelatin films (Yaewon Park, 2020)	19
Figure 11: A) Vascular structures fabrication using agarose as sacrificial material, B) Vascular network printed in suspended hydrogel, C) 3D bioprinting whole heart containing major blood vessels. A) (C. Norotte, 2009) B) (T.J. Hinton, 2015) C) (N. Noor, 2019).....	19
Figure 12: A) Hierarchical structure of natural bone. B) CAD model of 3D printed bone tissue engineering scaffolds with a gradient interconnected porosity. (Xi Chen, 2022).....	20
Figure 13: Surface morphology of printed scaffolds with varying rod-distances (μm): (a) 1000, (b) 600, (c) 420, (d) 200, all images have the same magnification, and scale bar (right) equals to 1 cm. (Hanxiao Huang, 3-D printed porous cellulose acetate tissue scaffolds for additive manufacturing, 2020).....	21
Figure 14: Bioprinting: Building the Future of Medicine, Layer by Layer (Bowen, 2020	22
Figure 15: Creality 3D 42-34 stepper motor and datasheet of capabilities presentation. (Figure provided by Grobotronics.gr)	25
Figure 16: Creality ender 5 pro 3D printer. Zoomed in figure shows the standardized part where the bioprinting head will be placed on (Figure provided by Creality.com)	27
Figure 17: Presentation of a 3D modeled parts showing in blue lines the 2D surfaces it was created from	28
Figure 18: Rendered standard view of bioprinting head assembly	29
Figure 19: a) Drive gear - 10 teeth helical gear. b) Move gear - 30 teeth helical gear.....	30
Figure 20: a) SKF ball bearing 628-8 2RS (Figure provided by SKF.com). b) Lead screw T5, 150 mm pitch 1 lead 2 (Figure provided by Grobotronics.gr).....	30
Figure 21: DATASHEET for ball bearing 628/8 -2RS showing the design specifications for the ball bearing to be placed in (Figure provided by SKF.com)	31
Figure 22: Move gear connection with lead screw nut, lead screw, and ball bearing for optimum alignment and friction minimization.....	31
Figure 23: a) Piston cap made from natural PLA for sterilization requirement. b) Syringe cap but in rendered mode. c) 30 T5 Gear holding cap for optimum alignment and stabilization of the gears. d) Vertical tunnel guide for lead screw clamp to vertically move.....	32

Figure 24: a) Filament PLA flex for the 3D printing procedure (Figure provided by grobotronics.gr). b) Optimum quality printed structure of the drive gear. c) Last few layers before the completion of the bioprinting head mount. d) 3D printing procedure of move gear 33

Figure 25: a) First physical assembly of the mechanism. b) Focused view for syringe attachment and calibration 34

Figure 26: Cropped view of firmware where using '/' the thermal safety factors are turned off 35

Figure 27: a) Visible powder portion of Cellulose Acetate. b) Solution in sealed container c) Bioink placed in the syringe for the first few seconds. d) Issue created on the top level of the bioink. Captured air creates a volume where pressure is not stable 36

Figure 28: Figure of different categories of standardized syringes. Based on the color, gauge and inner diameter are given for the calculations..... 37

Figure 29: First bio printed scaffold. Failed print caused of trapped air and flow rate miscalculation 38

Figure 30: a) By inverting the syringe, trapped air ventilates and after 5 minutes rest, air bubbles disappear. b) Attaching a conical 22-gauge tip for tests..... 39

Figure 31: a) Bioprinting test 1 (failed, creation of trapped air bubbles, flow rate miscalculation, no size accuracy. b) Bioprinting test 2 (formed structure but flow rate was miscalculated again). c) Bioprinting test 3 (achieved printing dimensions, accurazy in creating rectangles, flow rate optimization and surface of bed affected the printability) multilayer structure of 16 layers. d) Bioprinting test 4 (solid form, requirement of further flow rate optimization, printing speed optimization and calibration of bed) 40

Figure 32: a) Based on bioprinting test 4, rod distancing was calculated 700 μm b) Biorpinting test from literature above mentioned, 1000 μm rod-distancing..... 41

Figure 33: Modification in Gcode in order to deliver optimized results from mixture of Cellulose Acetate 25wt%, mixed with alizarin red powder for observation while extruding the lines..... 41

Figure 34: a) Cellulose Acetate 25wt% - 10 layer scaffold with rod-to-rod resolution 400 μm b) Cellulose Acetate 40wt% - 10-layer scaffold with rod-to-rod resolution 300 μm (woodpile architecture) 42

Figure 35: Cellulose Acetate 25wt% - 10-layer scaffold with rod-to-rod resolution 400 μm . Provided by University of Crete via SEM imaging 42

Figure 38: Difference in surface texture and structure of scaffolds. a) Top view placement b) Inverted scaffold view (both scaffolds where made from a CA 25wt% solution) 44

Figure 39: Morphology of the surfaces seems to not affect the cell-proliferation in day 1 in a visible level (both scaffolds where made from a CA 25wt% solution)..... 44

Figure 40: a) Maximum user-caring CA 25 wt% 10-layer scaffold presenting a uniform architecture. b) No user-caring CA 25 wt% 10-layer scaffold presenting irregular architecture 45

Figure 41: Observation of cellular responses such as adhesion and proliferation through the a) user-caring and the b) no user-caring 3D scaffold. 45

Figure 42: Bioprinting process of a Cellulose Acetate – Gelatine 10-layer scaffold..... 46

List of tables

Table: 1 Numerical calculations for analyzing 1 mm vertical movement on the Z-axis.....	26
Table: 2 Numerical calculations for whole 40mm vertical movement and motor efficiency indication	26
Table: 3 Portions of mixtures for trials	36
Table: 4 Printing calculations for optimization of Gcode.....	37

Chapter 1: Introduction

Regenerative medicine

Regenerative medicine tends to be the new trend in modern medicine these years, presenting great prospects in its development. Various definitions have been created over the past years from scientists to define the advancements of this science, what it stands for, and to focus on receiving the funds to further develop it.

An accurate definition of what Regenerative medicine stands for is given by (Daar & Greenwood, 2007), proposing that '*Regenerative medicine can be considered the next step in the evolution of organ replacement therapy*'. By the combination of other sciences such as biology and mechanical engineering, it does not only provide a replacement of the malfunctioning part of the body but also pre-constructs it by using the same biological material in a way that the body will absorb and accept it like it was never damaged. Furthermore, in vivo repairs could help the body to regenerate and help itself by guiding ideally the capabilities of the cells.

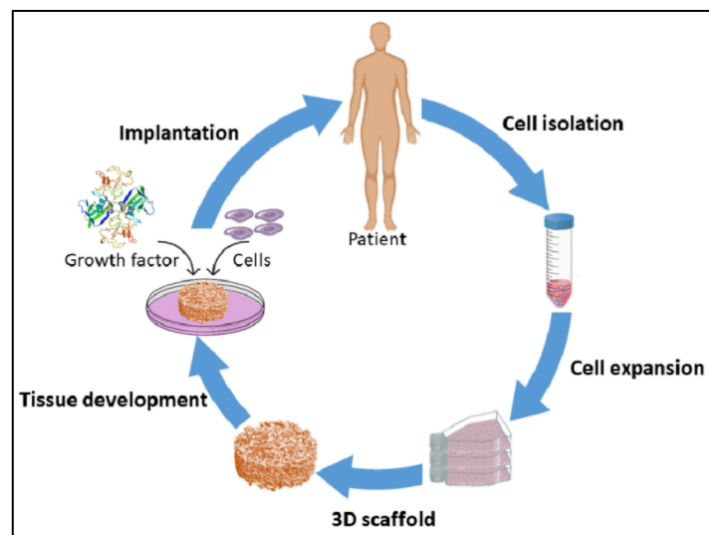


Figure 1: Circle of tissue engineering by (Asadian, 2020)

Tissue engineering

In the field of research and clinical applications, regenerative medicine aims to repair, replace, or regenerate cells, tissues, or organs from malfunctioning factors, disease, trauma, or aging. One of the most popular sections of regenerative medicine is tissue engineering which most of the time accompanies the definition of regenerative medicine. Tissue engineering could be defined as the guideline for regenerative medicine as it combines technical advancements from science fields such as material science, cell, and developmental biology, nanotechnology, and rapid prototyping (Prafulla K. Chandra, 2020)

Tissue engineering: Biomaterials

A wide variety of technologies has been developed over the years to evolve the field of regeneration medicine and tissue engineering as it was a completely new part of medicine when it first appeared. From the field of material science, naturally derived biomaterials such as collagen, fibrin, gelatin, and polysaccharide-based biomaterials such as cellulose, alginate, and glucose were introduced (Fa-Ming Chen, 2015) and developed as a tool that fights the risk of harming the body while operating, or a factor to help create a proper environment for cells to proliferate and differentiate in vitro, such as in a lab incubator. (Prendergast, 2020,)

Bioink	Cell Type/Tissue
Alginate	Chondrocytes/Cartilage
Agarose	hMSCs
Collagen	Chondrocytes
Fibrin	Hepatocytes/Liver
	hMPCs/Skeletal Muscle
	HUVECs/Vascular structures
Gelatin	hMSCs/Bone
	hMSCs/Cartilage
Gellan gum	Chondrocytes/Cartilage
	Osteoblasts/Bone
Hyaluronic acid	Fibroblasts
PEG	hMSCs
	Fibroblasts
Tissue-derived ECM	SCAP/Dentin
	Kidney

Figure 2: Bioinks referred to the Cell type/Tissue that they can regenerate

Tissue engineering: Cells

Another important field of science that contributes to the development of regenerative medicine and tissue engineering, is the field of biology. Biologists are responsible to research and developing ways to manipulate cells, helping them to proliferate and differentiate into specific categories of cells such as liver cells, nerve cells, muscle cells, intestinal cells, blood cells, stem cells, etc. By knowing the way to guide the cells to differentiate, in vivo applications would be a whole new era of medical operations.

Tissue engineering: 2D – 3D – 4D bioprinting

Finally, engineering is a wide field of science that could contribute to solving problems medicine could never. Engineering can offer solutions by making further technical research on the problem, designing mechanisms or tactics to solve it, even analyzing the problem technically to find a solution out of the box. A recent and well-developed contribution to tissue engineering is the development of 2D -3D – 4D bioprinting machines.

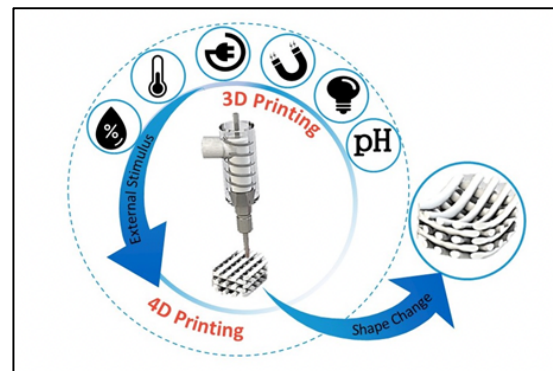


Figure 3: Illustrative diagram representing the addition of a pre-designed stimulus to promote a desired change at the construct. (Morouço, et al., 2020)

Arriving from its name, tissue engineering is based on creating conditions for tissue to regenerate or self-heal but there could be other applications such as culturing cell lines while guiding them to differentiate and proliferate which would be as efficient as regeneration and self-heal. By combining material science, biology, and engineering, a combination of problem-solving parameters is being created. Well-designed biomaterials, compatible to the cell lines are placed in a 2D – 3D – 4D bioprinter, and the production of a structure called scaffold is delivered.

Scaffolds in medicine

More specifically, a scaffold in the industry is a geometrical structure that consists of cylindrical rods or other geometrical objects that are bonded together, creating the outer shell of the constructing structure. Moreover, they are used to hold and accommodate the same or different material to produce the final structure without difficulties or misfiring. In other words, they could be called the external case for the inner construction.

Scaffolds in medicine are following the same geometrical strategy. The main target is to create a proper environment for the cells to be placed to differentiate and proliferate. In other words, scaffolds are used for tissue fabrication (Ma, 2004). For example, by using a 3D printer, a construct of cylindroid rods could be deposited line by line and layer by layer, to finally deliver a 'tic tac toe' 3D structures with square-like pores. If the mechanical properties are ideal and the 3D printed material is biocompatible, cell lines could be deposited and culture of them could be observed under the microscope.

Biofabrication

As mentioned above, bioprinting is a method of biofabrication that has piqued interest in the past years, and this is caused because of the efficiency and compatibility it has. Bioprinting is a simple but well-designed biofabrication method that brings the revolution in tissue fabrication. Bioprinting is categorized in the additive manufacturing sector, though it has a variety of techniques on how to fabricate the structure. Such techniques are the fused deposition modeling (FDM), the stereolithography technique (SLA), or the electrospinning fabrication technique. All three of them are categorized in additive manufacturing techniques but different technology and engineering are used to produce scaffolds.

Fused Deposition Modeling

Fused Deposition Modeling (FDM) has recently been one of the most trending techniques of 3D printing. These printers extrude filaments made by thermoplastic materials, providing a variety of mechanical properties to the final structure. The procedure is basic engineering. The filament in solid cylindrical rod form is being pushed by a rotating gear mechanism into a tube guiding the material into a nozzle where thermal energy is being applied, turning the solid cylindroid rod filament into a fluid. The thermoplastic fluid is being deposited on a surface called 'bed' while rotating motors are making guided movements to create a motif of lines. Line by line, layer by layer, based on the parameters given to the printer, the deliverance of a geometrical structure is presented in solid form. This phenomenon happens because while the thermoplastic material is being extruded at about 200 °C, room temperature at about 20 °C reacts with the hot fluid and gets it back to its solid form. (Ankita Jaisingh Sheoran, 2019)

Computer-aided design

All the above-mentioned fabrication methods are machines assembled of mechanical parts where electronic equipment has been installed on their assemblies to transform them from mechanisms to automation. Automation is a mechanism that no longer needs the human factor to operate but uses electronic signals given from a computer which guides it to execute the macro command. Computer-aided design is a method of 2D – 3D – 4D design in a computer unit that lets the user create an exact model of what he/she firstly had in mind. Those programs significantly evolved the industry technologically, financially, and innovatively.

A computer-aided design model can be used for simulation or finite element analysis, for a product design or development, and of course as a guided command for its creation. The guided command is also called the Gcode, a language written for these machines to understand and create significant design structures. Gcode is a developed binary language that coordinates and sets the parameters for the printer to execute. Linear movement, extrusion speed, printing speed, extrusion temperature. These are only a few of the commands Gcode provides the printer to create a perfectly executed line by line, layer by layer structure which offers mechanical properties and strict geometrical parameters. (W. Sun, 2005)

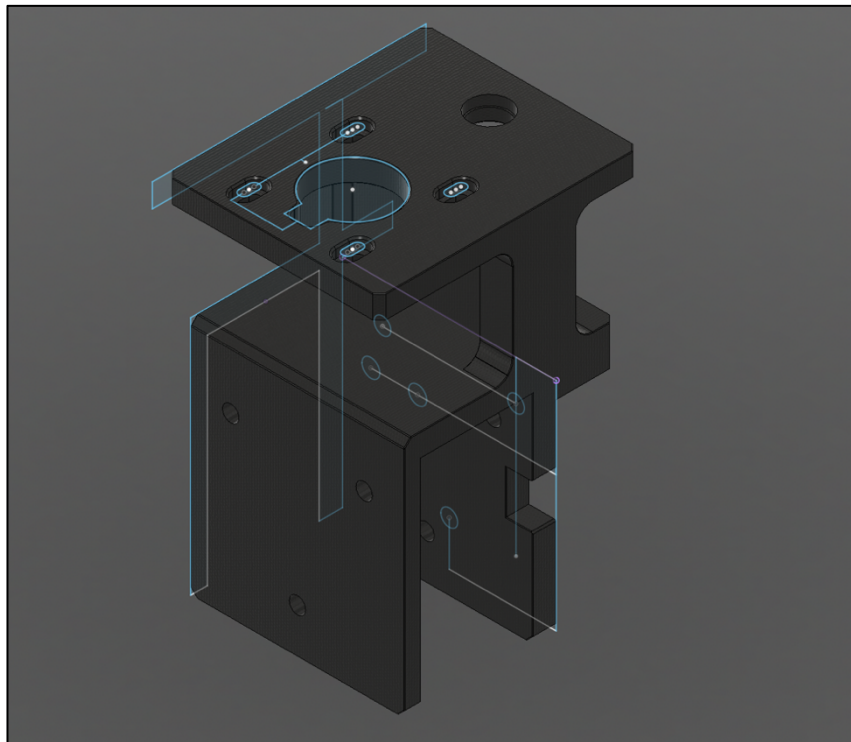


Figure 4: Standard view of a designed 3D model. Blue lines indicate the 2D sketch design and then by command extrude the 2D bulks into 3D (Illustration by author)

Thermoplastic materials

Standardized 3D printers use a variety of thermoplastics based on the properties the user prefers. Thermoplastics are plastic polymer materials that can become fluid or semi-fluid when their temperature raises drastically, and they solidify upon cooling. Most of them are inexpensive but could offer great results for hobbyists or even for industrial use. Some of the thermoplastic materials standardized 3D printers use are Polylactic acid (PLA), Nylon, Acrylonitrile butadiene styrene (ABS), Polycarbonate (PC), etc. Each one of them differs from the other, sometimes on the price, the thermal ability, or the mechanical properties upon creating the structure. As mentioned above, to create a specific structure, they first must melt and then get extruded into lines that construct the structure, the figure, or the scaffold, based on the CAD that instructed the 3D printer.

3D – 4D Bioprinting

Bioprinting could be considered one of the most innovative ideas in modern medicine. When 3D printers got into the market, their main use was suggested to be rapid prototyping, small-scale assembling, and material testing. Though, all that trend on 3D printing made companies focus on better results and more accurate manipulation of the machines and the materials which were used as filaments. The industry started using 3D printers for simulation analysis, for rapid prototyping which lowered the cost of research and development but also for commercial purposes too. While regenerative medicine and tissue engineering were making their first steps and development, 3D printing tended to be an efficient idea to experiment with. After all, tissue regeneration and self-healing could happen by attaching a small pad with differentiated cells on a wound and letting them coordinate on advancing regeneration and self-healing.

Biomaterials

It may seem unproblematic to transfer from a standardized 3D printing method to a 3D bioprinting one, but it is not. Unlike thermoplastics which get in a fluid form and then they turn back to a solid form, biomaterials differ in their properties. They may come from the same category, such as the protein-derived biomaterials or the polysaccharide-derived biomaterials but their mechanical or dynamic properties may differ. Those materials can be found in their purest form in an organism, surrounded by other materials and compositions. They have a semi-gelatinous form which provides them the ability to get involved with other materials and substances to operate organic operations for the integrity of the living organism.

3D – 4D Scaffolding

The definition of 3D – 4D scaffolding is commonly referred to as the same geometrical structure of a printed part but with different properties. Those can be differences either in the mechanical properties or the dynamic properties of the material and its printing method. For proper research guidance, the term 3D will be used for structures that hold their geometrical structure without any deformation. In addition, the term 4D will be used for structures that can change their geometrical structure because of their gelatinous form but without permanent deformation. In other words, 4D is a structure that is capable to change using a time parameter.

Chapter 2: State-of-the-art

Additive manufacturing is showing great development over the last decade. 3D printing has been the most famous additive manufacturing technique, taking place in a variety of applications in product development, rapid prototyping, and specialized manufacturing. By the development of the technique, applications such as architecture, industrial design, aerospace, and medical industries are only a few who based their research and development in 3D printing. More specifically, the simplicity of using a 3D printing machine led medical applications to develop and offer new solutions and innovative future ideas. 3D printing can be achieved by different methods, such as fused deposition mechanisms, stereolithography, electrospinning, and others. The fused deposition mechanism method is the simplest and seems to have great potential on its future development. This is where regenerative medicine and tissue engineering appear, promising a great future for the development of medicine.

The first few medical applications of 3D printing were for transplantation purposes of visualization of tissue and bone structure of the organism. Surgical operations have been a risky and time-sensitive procedures providing the surgical operator a great amount of stress and focus which exhausts him/her. New 3D printed body parts for visualization and tests purposes have been created for the operator to practice on, saving risk and time for the real operation. This is happening because each organism is unique anatomically and organically. That concludes to time efficiency, low-cost bio model production, and provision for surgical rehearsals, making 3D printing a novel technique for the development of medicine. (Cho Ki-Hyun, 2020).

3D printing sparked the interest of various scientific fields for its potential and innovation. Scientific fields such as Biology, Material science, and Engineering started focusing on developing methods for transplantation, reparation, regeneration, and self-healing for cells, tissues, organoids, and organs of organisms. By the combined effort of these scientific fields, novelty materials and structuring methods can provide with innovational transplantation and risky-free surgical operations, but also treatment of serious medical diseases.

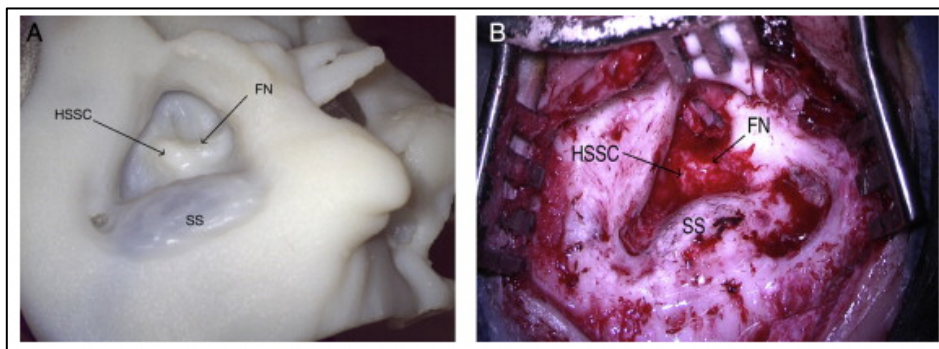


Figure 5: A) 3D-printed temporal bone model following dissection for pre-operative surgical simulation. (B) Intraoperative photo for comparison status post-CWD tympanomastoidectomy, demonstrating the horizontal semi-circular canal (HSSC), the sigmoid sinus (SS) and facial nerve (FN) (Rose, et al., 2015)

One specific construction structure 3D printing offers to tissue engineering is the so-called scaffold. Scaffolds are 3D modeled geometrical structures which are printed in different shapes via the 3D printer, providing a structure for the missing bone, cartilage, or skin to be replaced and reconstructed by the cells of the organism. Those scaffolds could offer in vitro or in vivo applications, by culturing cell-lines in them, helping them proliferate and differentiate using growth factors and by taking advantage of the architecture of the constructed scaffold. Thus, 3D printing is limited in creating scaffolds made by thermoplastic materials such as (PLA, ABS, PC, NYLON). By using the fused deposition mechanism technique, thermoplastic filament gets heated in temperatures of about 200 °C and the fluid is deposited line by line, layer by layer, constructing a scaffold.

Those materials often offer biocompatibility, based on their category and mechanical-dynamical properties. Unfortunately, tissue fabrication is a complex and multidimensional process. For example, biocompatible Polycaprolactone scaffolds were constructed for bone tissue engineering because they offer manipulative physical properties, and by the use of silver nanoparticles they developed antimicrobial properties for a successful tissue growth. (Radhakrishnan, 2020)

Thus, the tissue fabrication is not referred only to solid structures like the bones. Liver, cardiac, or neural tissue fabrication require a more flexible scaffold with different mechanical and dynamical properties. Gelatinous, flexible structures, with different porosity would be available to create an environment capable for proliferation and differentiation of the planted cells into liver, cardiac, or neural cells and create a successful scaffold.

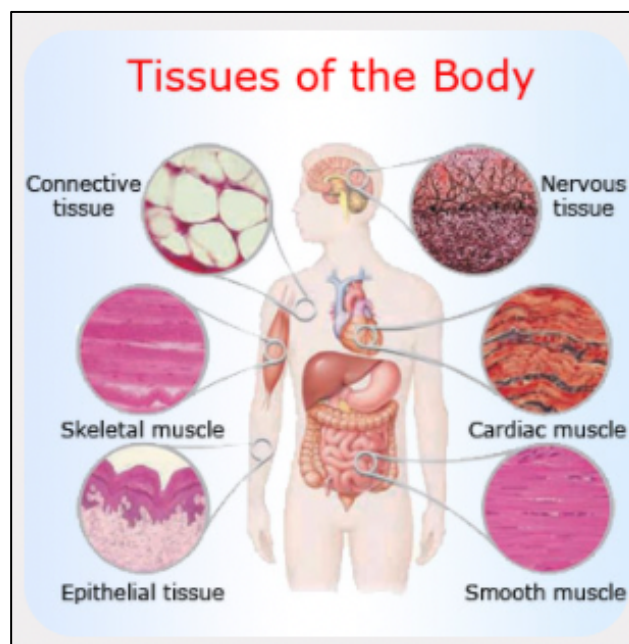


Figure 6: Tissues vary in their structure, function, and origin. (Simply science, n.d.)

Creating a gelatinous and flexible scaffold means that different materials had to be used. By the contribution of biology, material science and engineering, biologically derived materials such as collagen, fibrin, alginate, cellulose, etc., were presented to the world of 3D printing. This time though, because of their mechanical and dynamical properties those materials could offer 4D structure capabilities. Usually, 4th dimension in 4D printing is used as a parameter of time. That means that the scaffold or the structure can change its volume or geometry, based on the interfering phenomenon.

Such phenomenon, is the volume taken by the proliferation and interactions with the cell-lines which develops the scaffold to a different geometrical structure, a scaffold with gelatinous form changing its geometry by its elasticity, or a 2nd phase method of subtractive manufacturing, creating various porous sizes into the scaffold for the ease of cell culturing. By having that opportunity, different tissue fabrications could be expected, using the optimum parameters and guidance for the properties of the scaffold and the cultured cell-lines.

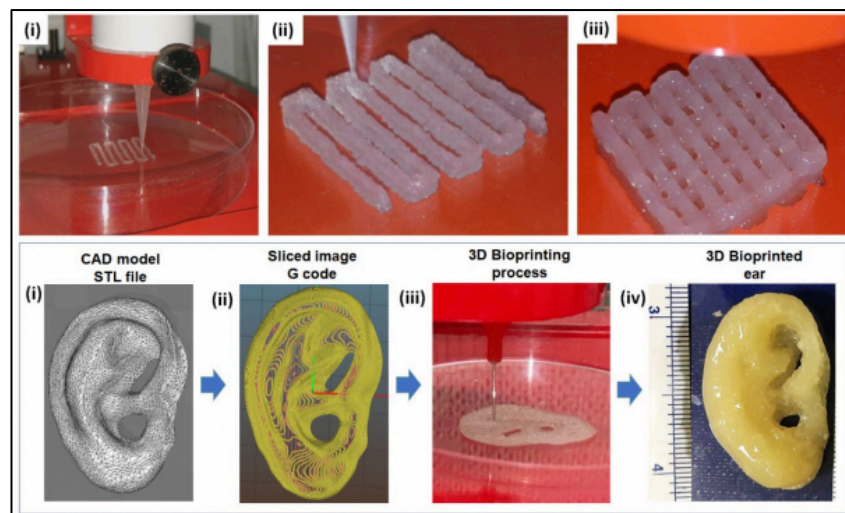


Figure 7: Print fidelity of the ink showing (A) printing of grid-like structure (i) extrusion of the ink through the nozzle, (ii) initial few layers, and (iii) formed grid-like pattern; (B) fabrication of human anatomical ear (i) CAD model and generated STL file, (ii) generated Gcode using slicer, (iii) printing process, and (iv) printed ear structure

These biomaterials are not coming filaments though. They are first taken in powder or liquid form, mixed with other solutions, creating bioinks. Those bioinks are most commonly used in a fluid form which means that a bioprinter is needed in order to perform the task. These bioprinters could be standardized by companies commercializing them or they could be made by the conversion of a standardized 3D printer. The only difference is that the bioprinter is using fluid mixture which means that there is no need of hyperthermal strain. A bioprinting head consisting of a syringe chamber for the fluid to be placed, and a piston mechanism for the extrusion of this fluid could efficiently function a bioprinter. There are various techniques for the fluid extrusion, based on choice.

There could be used a pneumatic-driven mechanism pushing air to extrude the bioink, a piston-driven mechanism doing the same thing but with mechanical force, or a screw-driven mechanism for extrusion through rotational displacement in case the viscosity of the fluid complicates the situation or continuous mixing of the bioink is required.

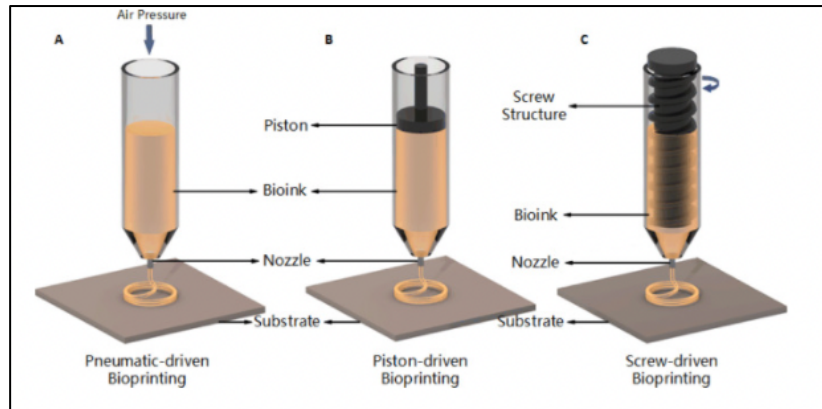


Figure 8: Extrusion mechanisms based on the requirements of the bioink (Zeming Gu, 2020)

Based on literature, 4D has been developing rapidly the last 10 years, providing with spectacular results in tissue and organ fabrication. Using bioprinters with different capabilities such as single or double extrusion mechanisms, different cross-linking procedures, and bioinks, a variety of results are presented and are still in developing progress. Interesting in vivo 3D bioprinting results of skin tissue fabrication are presented below, showing the additive manufacturing procedure, the pattern of the scaffold, image processing on the proliferation of the cells, and the application of the physical model on a patient.

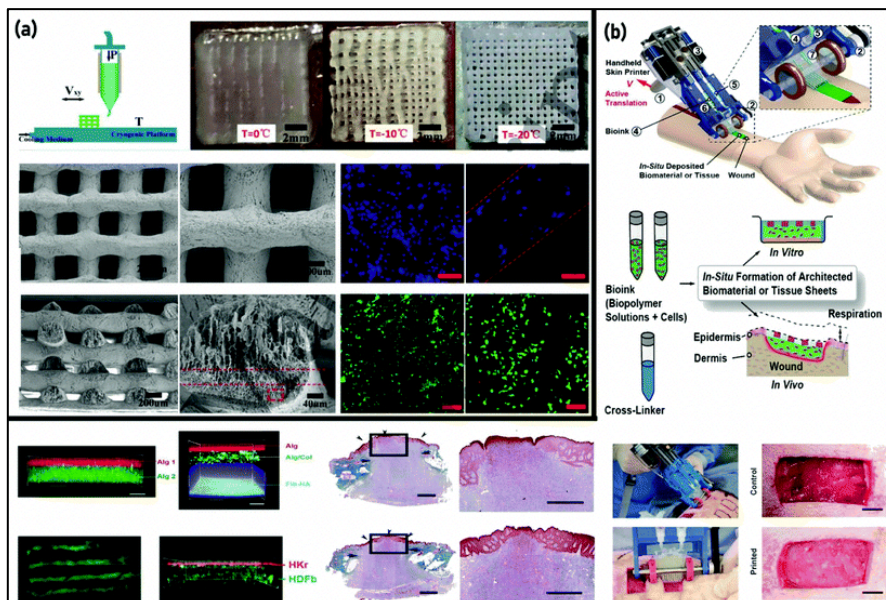


Figure 9: 3D bioprinting of skin tissue: Provided by (Askari, et al., 2020)

Another 4D bioprinting interesting construction is the development of automatic shape shifting scaffolds. Bioprinted scaffolds constructed by shape-memory polymers provide folding and unfolding properties, making them really important in drug delivery situations or creating a microenvironment for cell-lines to proliferate and differentiate. Those materials are thermal manipulative making them interacting differently applied in organisms temperatures of 37 °C in contrast with external room temperature. There are also materials that are electro-responsive making them capable to undergo changes on their properties when changes in electric potential stimuli occur. Another category are the water, humidity, or moisture responsive materials such as hydrogels which can change their geometry and fold into shapes that were pre-designed.

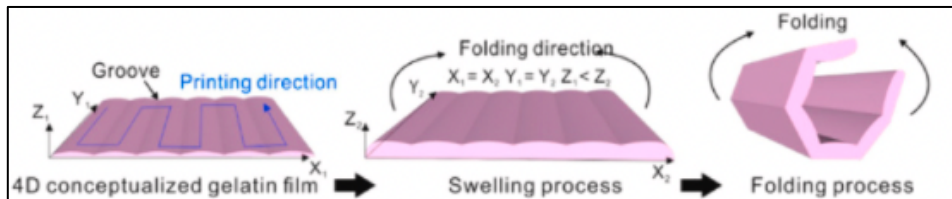


Figure 10: Folding mechanism of the gelatin films (Yaewon Park, 2020)

Moving on to another bioprinting fabrication, attempts for vascular structure fabrication using biomaterials as a sacrificial material proved to have a great potential and visual results could represent this. Using biomaterials such as agarose, hydrogels, and GelMA (Gelatin Methacryloyl), vascular structures, vascular networks, and even a heart containing blood vessels have been created and are being developed for potentially innovative results.

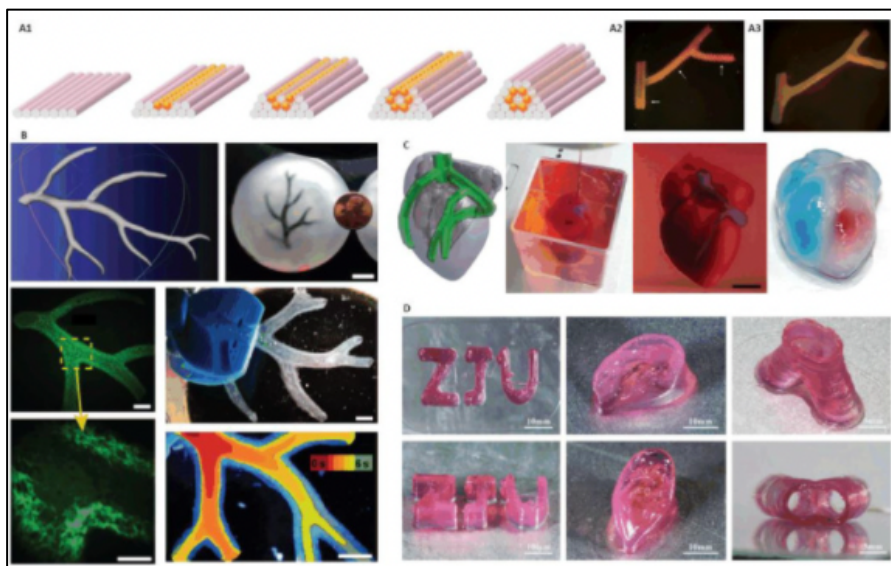


Figure 11: A) Vascular structures fabrication using agarose as sacrificial material, B) Vascular network printed in suspended hydrogel, C) 3D bioprinting whole heart containing major blood vessels. A) (C. Norotte, 2009) B) (T.J. Hinton, 2015) C) (N. Noor, 2019)

As known from bone tissue 3D printing, it has been challenging to create an environment for rapid and efficient healing of a large wounded area. This is caused of the lack of the essential bone extra-cellular-matrix. In order to create an environment such the ECM, 4D bioprinting takes places in the research by the construction of macro-micro structure to nano-sub nanostructure porosity inside the geometry of the scaffold, providing a gradient porosity environment for cell-laden placements to proliferate and differentiate differently, based on the size of the porous. By using additive manufacturing techniques or subtractive manufacturing techniques, such environment is possible to exist. Using modelling tools such as generative engineering, porosity can be manipulated in the 3D model and change, based on the preference of the expected result.

Thus, as much potential this research provides, a successful physical model is yet to be delivered because of the challenging parametric manipulation of biomaterials, FDM mechanisms, mechanical-chemical-biological stimuli, and complexity of organisms.

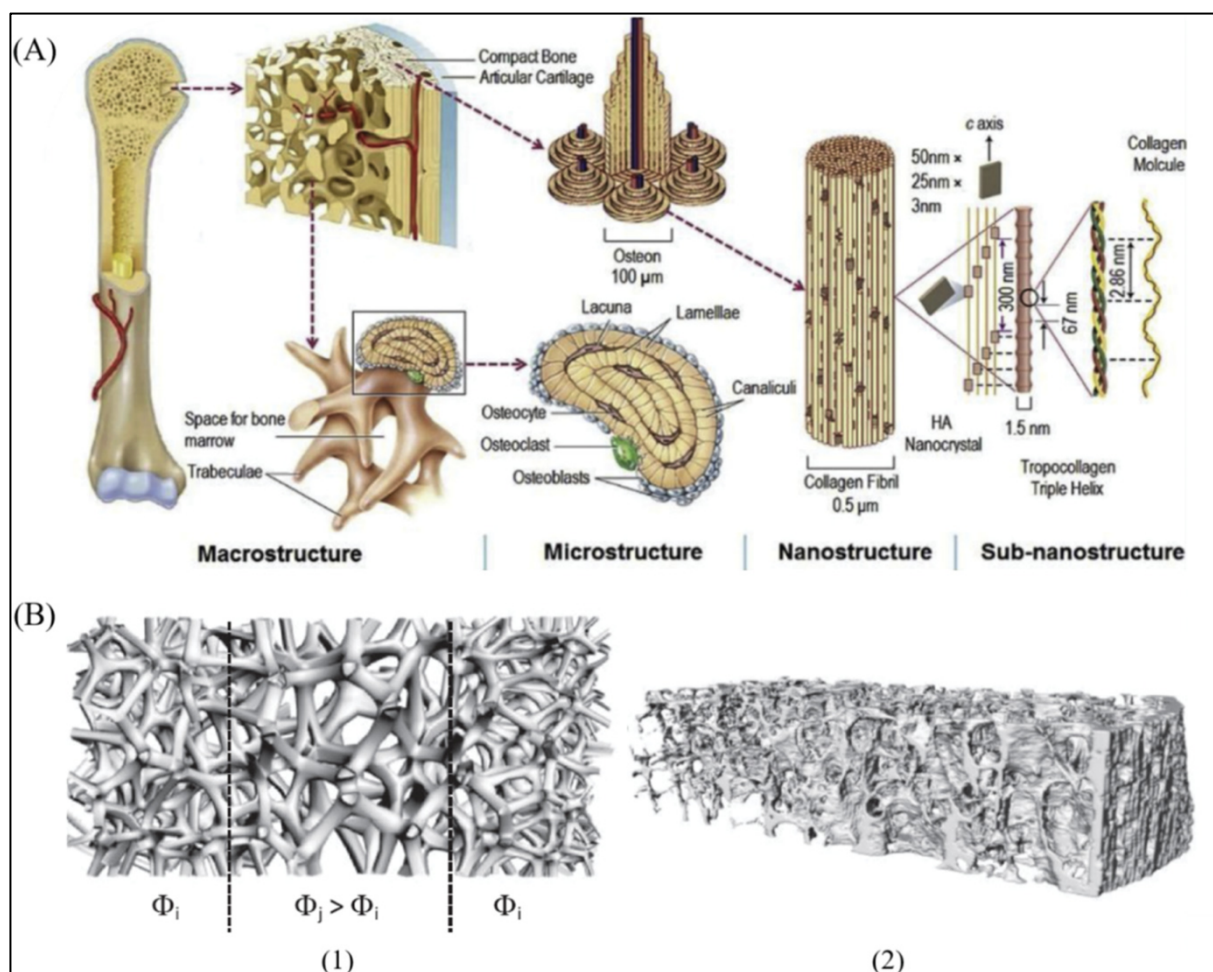


Figure 12: A) Hierarchical structure of natural bone. B) CAD model of 3D printed bone tissue engineering scaffolds with a gradient interconnected porosity. (Xi Chen, 2022)

As mentioned above, combining the scientific fields of biology, material science, and engineering, provides great knowledge and development in a variety of sectors. To be more specific though in the state of the art for this research, a bioprinting method and a biomaterial have to be chosen in order to focus on specific results and properties. From literature, choosing a fused deposition mechanism for the fabrication method and Cellulose for the biomaterial tends to provide us with more special results for the research of this thesis.

Cellulose Acetate has been known as a biomaterial with great properties manipulation and deliverable printability potential. From the literature, it is known that it is proved that Cellulose Acetate is a promising material in tissue engineering because it can provide with mechanical support, but also mimic the extracellular matrix (ECM) making it easier for cells to proliferate and differentiate. As a biomaterial, it can be mixed with other biomaterials and solutions in order to manipulate and differentiate its mechanical and dynamic properties. Variety of above mentioned applications support that Cellulose Acetate is a bioink which can be used in heart valve tissue engineering, achieving cardiac cell growth and proliferation, but also for tissue scaffold engineering of bone and skin. (Close P. Gouma, 2012), (M.N. Nosar, 2016)

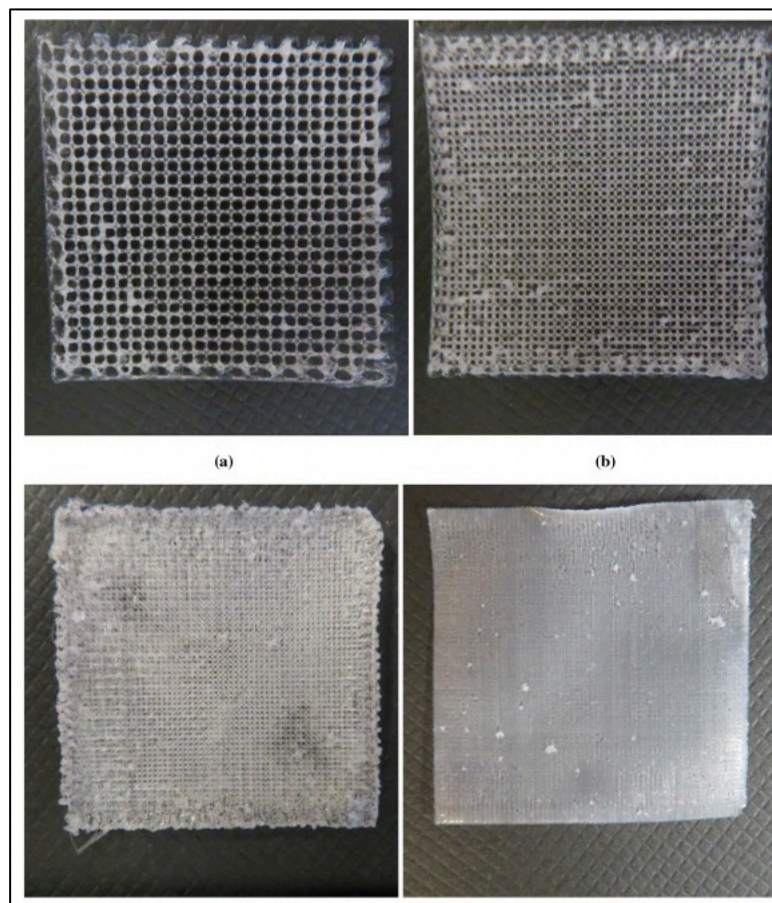


Figure 13: Surface morphology of printed scaffolds with varying rod-distances (μm): (a) 1000, (b) 600, (c) 420, (d) 200, all images have the same magnification, and scale bar (right) equals to 1 cm. (Hanxiao Huang, 3-D printed porous cellulose acetate tissue scaffolds for additive manufacturing, 2020)

In this thesis research, mixtures of Cellulose Acetate with Acetone will be prepared and tested in models designed in a computer aided design program, to deliver scaffolds with similar or better characteristics compared to the ones from literature. The research will reach three different stages to provide an all-in-one innovative solution for fabrication. The first step will be the conversion of a cheap (300 euros) standardized 3D printer into a 3D-4D bioprinter by constructing it mostly out of Polylactic acid (PLA) making it cost-effective for new scientists to penetrate easily into this scientific field. By following step by step, the conversion to a bioprinter is efficient and cost-effective, comparing to a standardized bioprinter being sold for more than 10.000 euros.

Saving time and research, the bioink used for the deliverable scaffold will be Cellulose acetate as above mentioned, because of its mechanical and dynamic properties. The selection of this specific material provides great potential for construction of optimum bioinks offering different properties (solid-forms or gelatinous). The third and final step is the parametric manipulation of the bioprinting settings and calculations which by further development will be able to deliver complex scaffolding geometries. Providing with instructions of every step for the conversion of the bioprinter, the reader will be able to use this thesis as a guiding manual to start his/her journey in tissue engineering. After all, solutions and innovations come from the cooperation of great scientists, combining their skills and ideas to create literature and results for future development.



Figure 14: Bioprinting: Building the Future of Medicine, Layer by Layer (Bowen, 2020)

Chapter 3: Research methodology

An important piece of this research will be the development of 4D scaffolding techniques for tissue imaging on them. 4D scaffolds were chosen over 3D scaffolds because of their ability to change over time and circumstances, allowing a more flexible environment for cells to proliferate and differentiate. As mentioned above, the challenges in bioprinting differ not only in their complexity but also in the scientific field. There are challenges that only biologists can solve, such as the complexity in the differentiation of the cells or the challenges in finding the perfect environment for them and their safety. (Gi Hoon Yang, 2019)

Challenges for materials scientists would be the creation of formulas based on biomaterials, to create an efficient mixture of bioink which would be easily manipulated by the preferences of engineers but on top of that, its cohabitation with cells is vital. Just as importantly, the field of engineering has the responsibility to take all the research from biologists and material scientists and create a functional mechanism-automation that could deliver the factor to make the experiment successful.

4D scaffolds have the potential to even turn into organoids or even organs. For this achievement, the mechanical and dynamic properties of the scaffold have to be completely manipulated and parametric. For this specific research, Cellulose Acetate is the material that was chosen because of its biocompatibility, the low cost as a material, and its mechanical and dynamic properties. From literature assistance, the preparation of a mixture for its use as a bioink is simple and effective. Mixtures of Cellulose Acetate powder (CA) and Acetone for printability tests will be made to find the best match for this research. Portions of 10,20,30 wt% CA will be mixed with Acetone separately for 5 minutes in the Speedmixer at 1700 RPM in sealed containers. After the stirring, a 5-hour rest will prevail for the acetone to mix with the CA powder and form a fluid. (Hanxiao Huang, 2019)

For the fused deposition mechanism, a standardized 3D printer and specifically the Creality 5 ender pro was bought for the lab tests. Though, the standardized 3D printer is pre-designed for thermoplastic filaments in a solid form. That means that a re-design of the printing head has to be made to change the way of extrusion. The cellulose Acetate mixture will be in a fluid form which means that the standardized rotating gear will not be able to deposit it into the nozzle chamber. For that reason, using a CAD program, a 3D re-designed model of a bioprinting head will be studied to take place of the standardized one.

The same philosophy will be used as the standardized one, operating stepper motors that rotate gears but this time, gears will work together to create a transmission ratio for a smooth movement. Instead of the thermal printing head, a commercial 5 ml syringe will be used as a bioprinting head. Along these lines, the Cellulose Acetate mixture (bioink) will be placed in the syringe in that remaining liquid form, and a custom piston will force mechanical pressure on the fluid which in turn will be extruded through the nozzle tip. (Konstantinos Ioannidis, 2020)

Scanning electron microscope imaging will be used as a technique for the observation of size and structure of the scaffolds. This observation tool will offer enough information to optimize the parameters of the bioprinter for optimum structure results. Furthermore, In-vitro cytocompatibility studies will take place to evaluate cell adhesion, growth, and proliferation.

Chapter 4: Research findings / results

Designing the bioprinting head

Arising from the needs of the above-mentioned requirements, there should be a re-design of the printing head of the standardized printer so that the extrusion will be based only on the pressure placed on the fluid and not on its conversion from one state to another (solid to fluid). The first step is to try and use as many standardized parts of the 3D printer as possible. Starting with the mechanism which will be placing pressure on the fluid, the stepper motor which was first used as a push-pull automatism for the guidance of the filament, will now have the role of a rotating gear that will be converting the rotational motion into vertical displacement. Assuming that there is a mount to attach the special parts of the bioprinting head, the need of a standardized syringe will be required. A custom piston that will make vertical moves into the syringe will be used as a moving part of the rotating gear where in turn, will be attached to the stepper motor providing the required rotation.

In case of need for a smoother conversion of rotating movement into vertical, two gear transmissions could be reached. This way, the first gear will be attached permanently to the stepper motor and will be named the drive gear. The second gear will be side by side to the drive gear receiving rotational movement and will be named as moving gear. By rotating the moving gear, a connection with the moving gear lead screw will be moving vertically achieving the push-pull mechanism the standardized 3D printer offered. This time though, the pressure will be dedicated to the fluid and not to the filament.

Lastly, an ergonomic and light-weighted mount has to be designed to attach all these moving and fixed parts. It is important to pre-assemble the bioprinting head before attaching it to the modified printer because nothing else will be changed except that. All the other parts of the printer will be used as they were supposed to. The reason this modification happens stands for the efficiency needed to make those tests. Taking one by one all these parts would require further research, calibration, and troubleshooting. By using the standardized 3D printer, the ablation of the standardized printing head and the attachment of the modified bioprinting test would provide results with less variety of troubleshooting parameters.

The most cost-effective method of manufacturing for the bioprinting head would be the use of the standardized 3D printer bought for the tests. Before removing the printing head from the assemble, good function tests had to be made to confirm the calibration of the structure. Rather than 3D printing commercial testing structures, the parts for the bioprinting head were printed several times for confirmation of good functionality. As mentioned in the previous chapter, Polylactic acid (PLA) is one of the most famous and commonly used materials for 3D printing because of its thermal sustainability and the substantial mechanical properties it offers.

Mechanism functionality calculations

Before the beginning of 3D modeling, there is a need for the requirements of the mechanism. 3D printing is based on many parameters working together for the best possible outcome. The same thing has to happen for the bioprinter to work efficiently. The basic parameters that have to get modified or transferred for the conversion of the printer are the capabilities of the stepper motor, the transmission ratio of the co-operating gears, and the vertical distance the piston has to go through for the deliverance of the extrusion.

Using the datasheet (information given from the manufacturer of a product) of Creality's extrusion stepper motor, the capabilities are presented below:



Figure 15: Creality 3D 42-34 stepper motor and datasheet of capabilities presentation. (Figure provided by Grobotronics.gr)

Another parameter for the implementation of the calculations is the distance the piston has to go through to extrude the fluid from the chamber of the syringe. The standardized 5 ml syringe has a height of 40 mm for the fluid to get extruded completely from the chamber.

Moreover, the lead screw has a pitch (pick to pick) distance of 1 mm, and also it is double-threaded which means that a complete rotation of the lead screw will vertically move the piston:

$$1 \text{ mm (pitch)} \times 2 \text{ (double – threaded)} = 2 \text{ mm per revolution.}$$

From the specifications of the stepper motor, it is known that 200 rotating steps of 1.8 degrees will provide a full rotation of the lead. The ender 5 pro 3D printer has pre-installed in its firmware a capability called micro-stepping. Micro stepping offers the ability to the stepper motor to do even smaller steps for a quieter and more manipulative movement. The number of standardized micro-stepping of this printer is 1/16. Applying all this information in an equation, parametric calculations are created as:

$$\text{Bioprinter steps per mm} = \frac{((\text{steps per revolution}/\text{ratio}) * \text{micro stepping})}{\text{lead screw pitch} * \text{double threaded}}$$

INFORMATION GIVEN (v2)		
STEP	=	1.8o
1 revolution (360o)	=	200 step
Lead screw PITCH	=	2 mm
Microstepping	=	1/16
Ratio	=	1:3
max revolutions per min = 1000		
Result = 4800 step = 1 mm on axis		

Table: 1 Numerical calculations for analyzing 1 mm vertical movement on the Z-axis

Now that the numbers are calculated for 1 mm vertical movement, another parametric board has to be created to calculate the whole desired vertical deposition movement in terms of steps.

Analyzing the parametric board above, by multiplying the whole vertical deposition of 40mm with 4800 steps (for 1 mm), 19200 steps will be needed for the piston to move from the upper level to the bottom level of the syringe. The next step is to calculate how many revolutions these steps are. The calculation for $\frac{192000}{200} = 960$ will be the revolutions needed for the whole movement.

Scenario for 2 gear calculations (ratio 1:3)				
Desired vertical deposition	=	40	mm	
4800	steps	=	192000	steps
192000	200	=	960	(revolutions)
960	1000	=	96,00%	
60	96,00%	=	57,60	seconds / 45mm -> for max efficiency stepper motor
60	4,5	=	115,20	seconds / 45mm -> for 50% efficiency stepper motor

Table: 2 Numerical calculations for whole 40mm vertical movement and motor efficiency indication

Though, from figure 4 above, the stepper motor can provide maximum revolutions per minute equal to 1000. That concludes 96% of the capability the stepper motor provides. The printing speed of the bioprinter will be far less than the calculated one which means that even if the motor provides energy for a 50% efficiency, the functionality of the extrusion will be stable and not demanding.

3D modeling of the bioprinting head

Computer-aided design programs have been developing at an advanced level for the past 20 years providing innovative solutions and methods for design in 2D or 3D. Those programs offer a wide variety of commands which not only saves time for the designers but also empowers them to be more creative and innovative. The program which was chosen for the research is AUTODESK FUSION 360. It is a program that not only offers the user a friendly designing platform for 2D – 3D, but it also offers simulation procedures, rendering for modeling presentation, and a mechanical drawing section for the engineer to present guidance for the manufacturer.

In the case of using a 3D printer, the last step is dismissed. That happens because after exporting the 3D model file, another program that is responsible for the communication with the 3D printer takes place. The program which mediates between FUSION 360 and the 3D printer is called a 'slicer'. This program is responsible for converting that solid form 3D model into lines and layers for the printer to understand and create step by step. The slicer not only 'slices' the 3D model, it moreover lets the user set parameters for the 3D printer, simulates the procedure for possible pre-troubleshooting, and also fabricates the Gcode for the guidance of the printer in its language.

Designing parts is always a complicated and dedicated procedure that demands traveling back and forth for the best possible outcome. To avoid changing the design of the parts several times, a standardized part where the printed head was mounted, got dimensioned for the new bioprinting head mount to be attached exactly based on these dimensions. Below, the Creality's ender 5 pro 3D printer and the specific part, which was dimensioned are presented, clarifying where the bioprinting head mount is going to be attached.

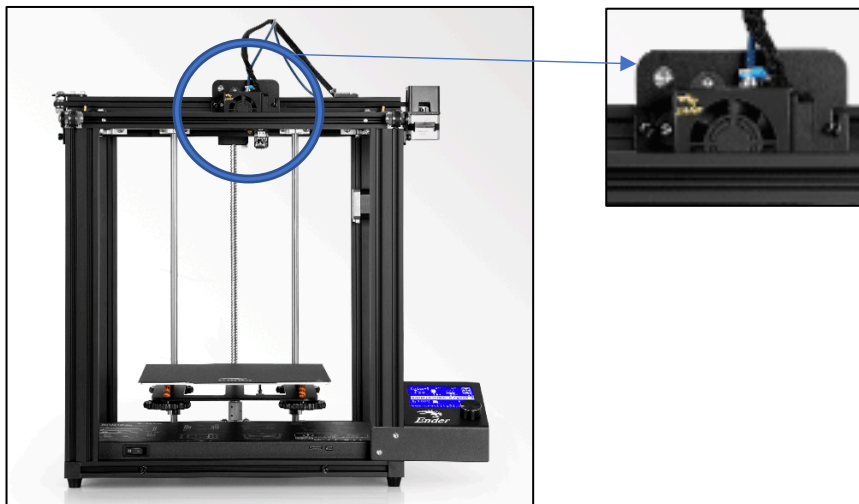


Figure 16: Creality ender 5 pro 3D printer. Zoomed in figure shows the standardized part where the bioprinting head will be placed on (Figure provided by Creality.com)

Presenting the 3D modeled parts

FUSION 360 is a designing program with advanced capabilities. While designing in a parametric environment, a pause for rendering could provide a better view of the mechanism. The figures presented below, are in the designing environment giving the reader of the thesis a better sense of hands-on designing.

As presented in the figures above, while designing in 2D surfaces, the part is developed to a 3D form based on the commands of the program. The most common commands are:

- Extrude (applies on a 2D surface, creating a 3D form because Z-axis is pulled)
- Hole (creation of holes and standardized threaded holes)
- Chamfer (Breaking sharp corners for better construction quality)

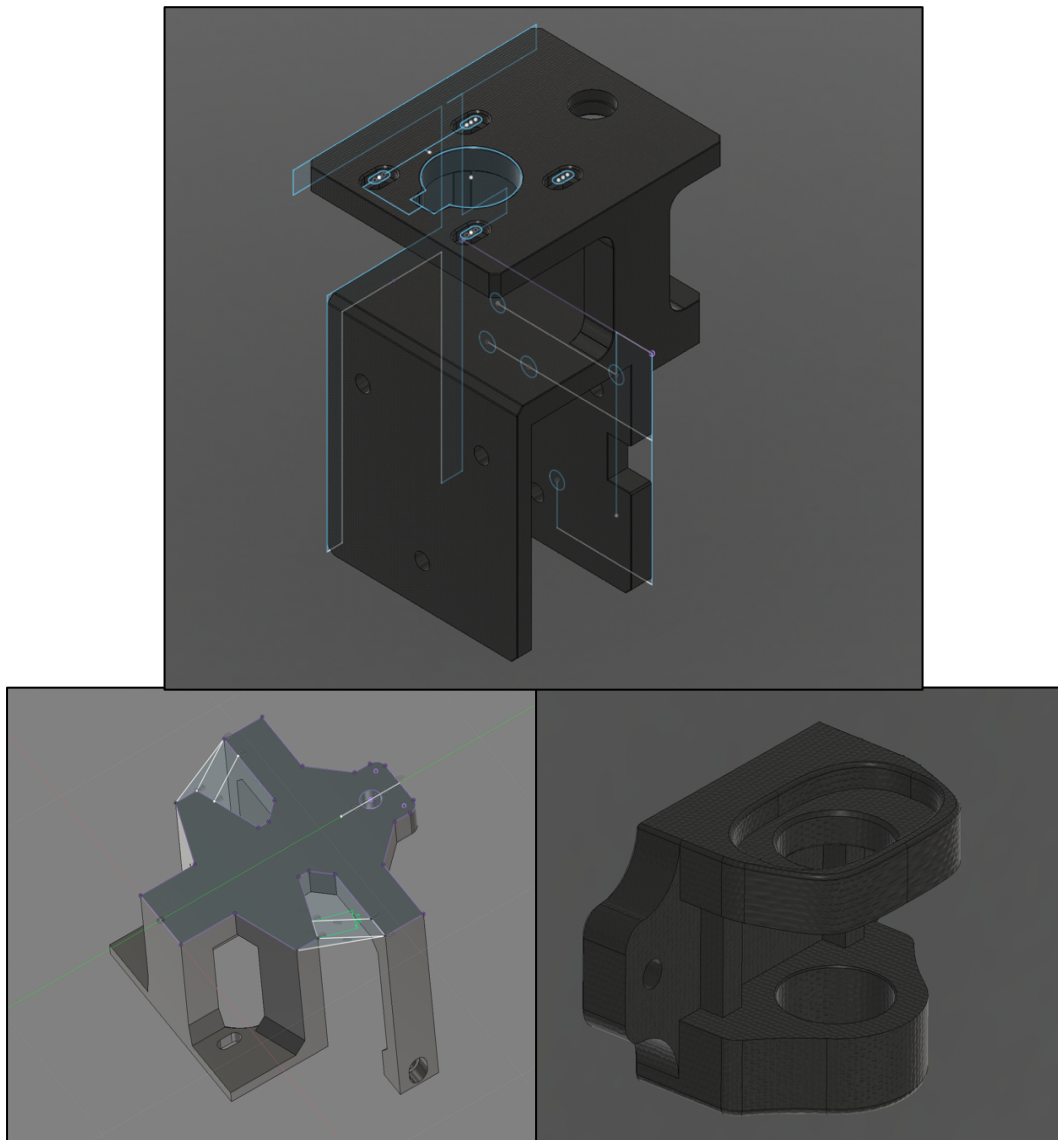


Figure 17: Presentation of a 3D modeled parts showing in blue lines the 2D surfaces it was created from

While finishing with the first stage of 3D modeling, an image rendering procedure begins to have a better understanding of the realistic model and its real-time design structure. Image rendering is a customizable section of CAD programs. The figures below present the final assembly (all parts attached) but also show renders for each part itself.

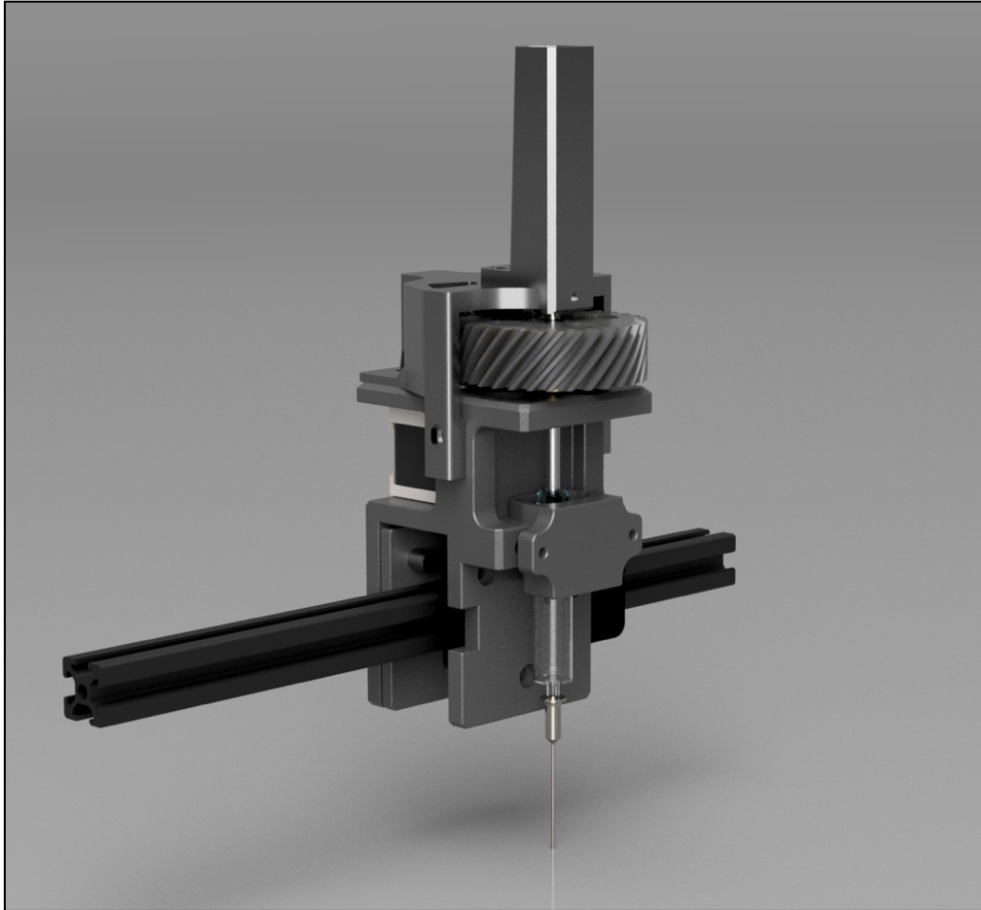


Figure 18: Rendered standard view of bioprinting head assembly

After designing each part, a new file called assembly was created where the user could place by-commands each part at the specific place it is demanded, in order to start creating the final structure of the model. The size of the simulated bioprinting head is 200 mm height x 80 mm width x 80 mm depth, making it a compact assembly. This would offer to the modified bioprinter a light-weighted bioprinting head that would not negatively affect the efficiency of the stepper motor. The size also offers steadiness without vibrations and an easy calibration step-by-step procedure.

Creating a structure completely by Polylactic Acid is not only a cost-effective procedure, but it also offers capabilities for standardized industry parts to be placed to the mechanism for better alignment and co-operation of the parts. The first standardized part which is going to be used for the mechanism is a lead screw T5 (diameter 5 mm) with pitch 1, single-threaded, and length of 140 mm. Another industrial part that is going to be used is a ball-bearing for the attachment a free rotation of the gear avoiding friction.

Continuing with the presentation of the parts that structure the assembly, the figures of the two gears are depicted below. From standardized gear modeling, three parameters are highlighted for efficient transmission and wear. It is best for the gears to have the same width, for the teeth to be intertwined without the creation of further friction and specific strain at edge points. The module indicates the size of the gear based on the reference diameter divided by the number of teeth. From literature $\text{module} = 3$ for this construction is greatly efficient.

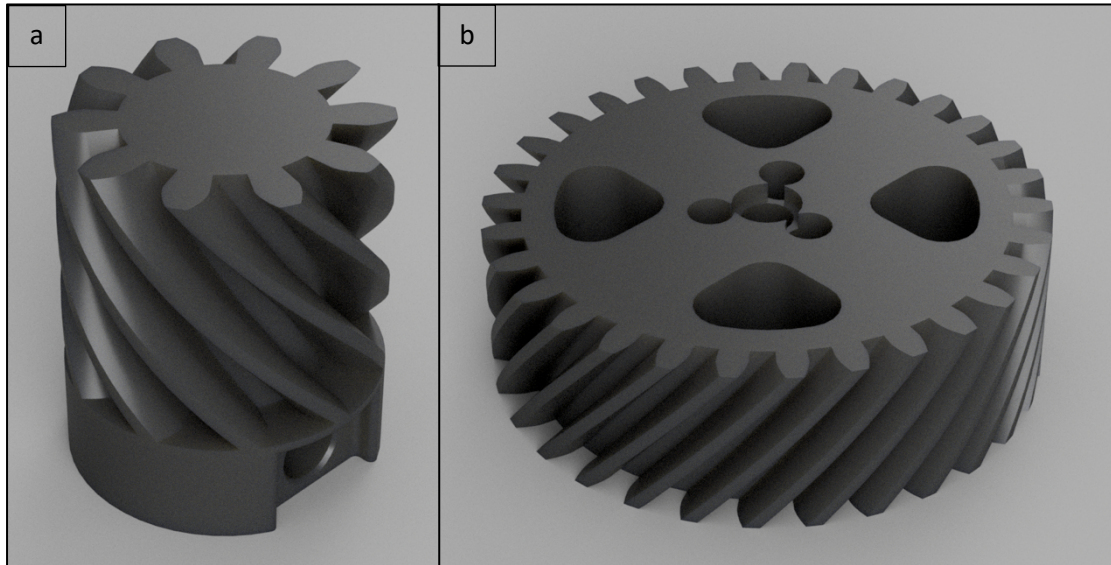


Figure 19: a) Drive gear - 10 teeth helical gear. b) Move gear - 30 teeth helical gear

Lastly, the complexity of the gear teeth often prevails the interlocking. Having the ability to construct this gear with a 3D printer, that acceptance does not have to be applied. 3D printing as an additive manufacturing technique offers complex geometries to be created in opposed to subtractive techniques such as computer numerical control (CNC) machines. Thereby, the gears were designed with 45-degree angled teeth, called helical gears, and offering better interlocking because of the larger contact surface teeth create.

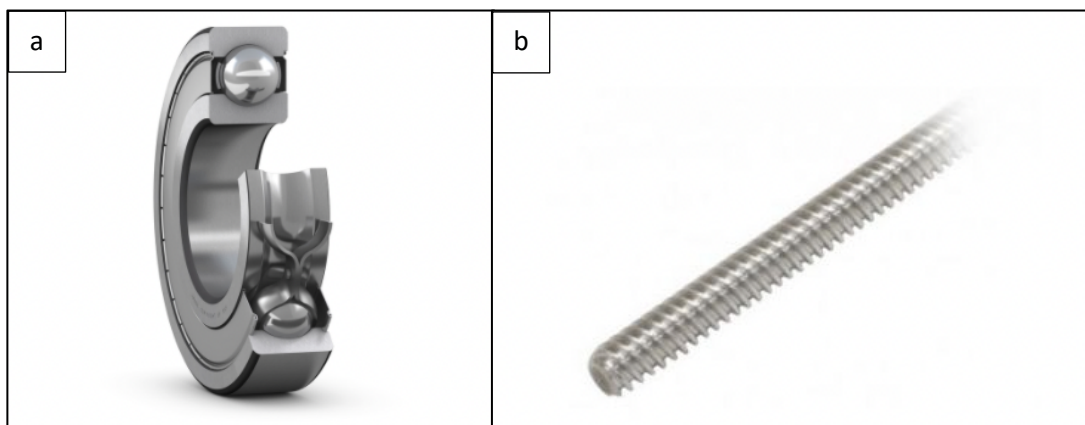


Figure 20: a) SKF ball bearing 628-8 2RS (Figure provided by SKF.com). b) Lead screw T5, 150 mm pitch 1 lead 2 (Figure provided by Grobotronics.gr)

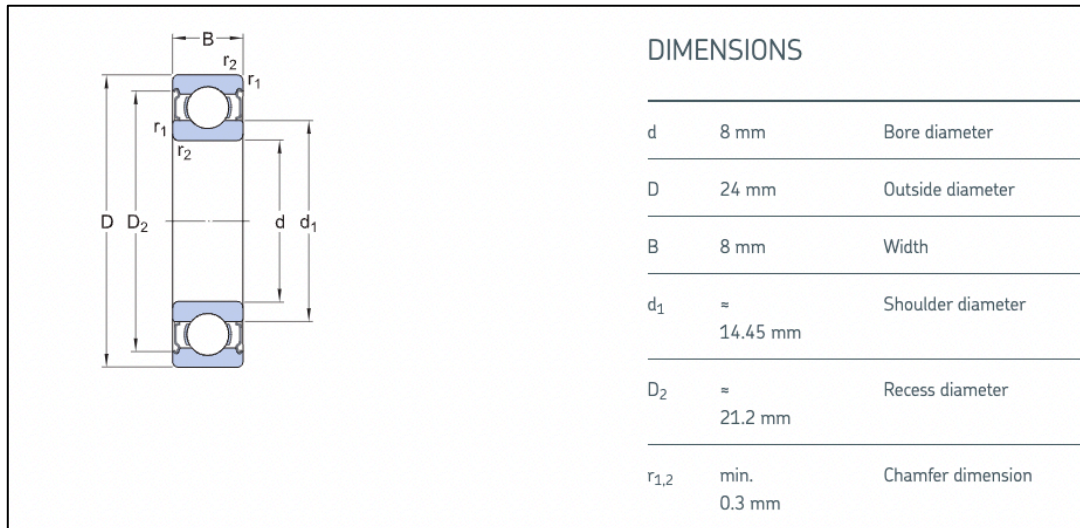


Figure 21: DATASHEET for ball bearing 628/8 -2RS showing the design specifications for the ball bearing to be placed in (Figure provided by SKF.com)

Based on the datasheet of the ball-bearing, model 628-2Z was chosen for the assembly because of its minimal dimensions and its mechanical properties. The mechanical properties that required that ball bearing, were the basic dynamic load rating $C=3.9$ kN and its Reference speed of 63.000 rounds per minute. Those properties were far greater than the required ones. Its low cost was the main reason and its use to minimize friction attached with the moving gear. From the figure above, the bore diameter of 8mm will be united with the lead screw nut, attaching the moving gear into the ball-bearing. This way, the friction will not affect the transmission ratio with losses.

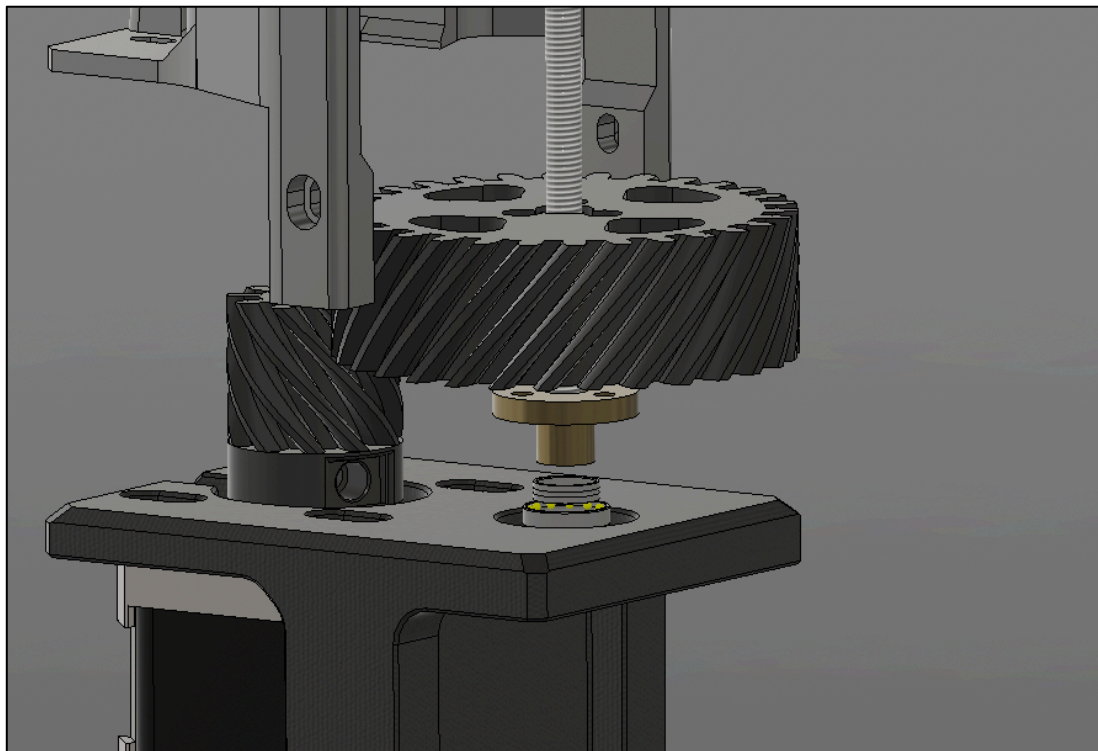


Figure 22: Move gear connection with lead screw nut, lead screw, and ball bearing for optimum alignment and friction minimization

Moving on to the parts rendering presentation, the creation of a custom piston had to be created to operate both with the syringe and the vertical movement of the moving gear. Also, a syringe clip was designed for the syringe to hold steady during the whole procedure and provide a better calibrating setup. The syringe clip is designed in a way to calibrate the syringe but also hold it still via the lip channel and the side holes which hold as one the syringe clip with the bioprinting head mount.

Furthermore, a gear holder cap with a channel for the lead screw was designed and from the projection of the lead screw channel, another tightening part was designed to hold the lead screw from rotating so that the rotation of the gear would vertically move it upwards and downwards.

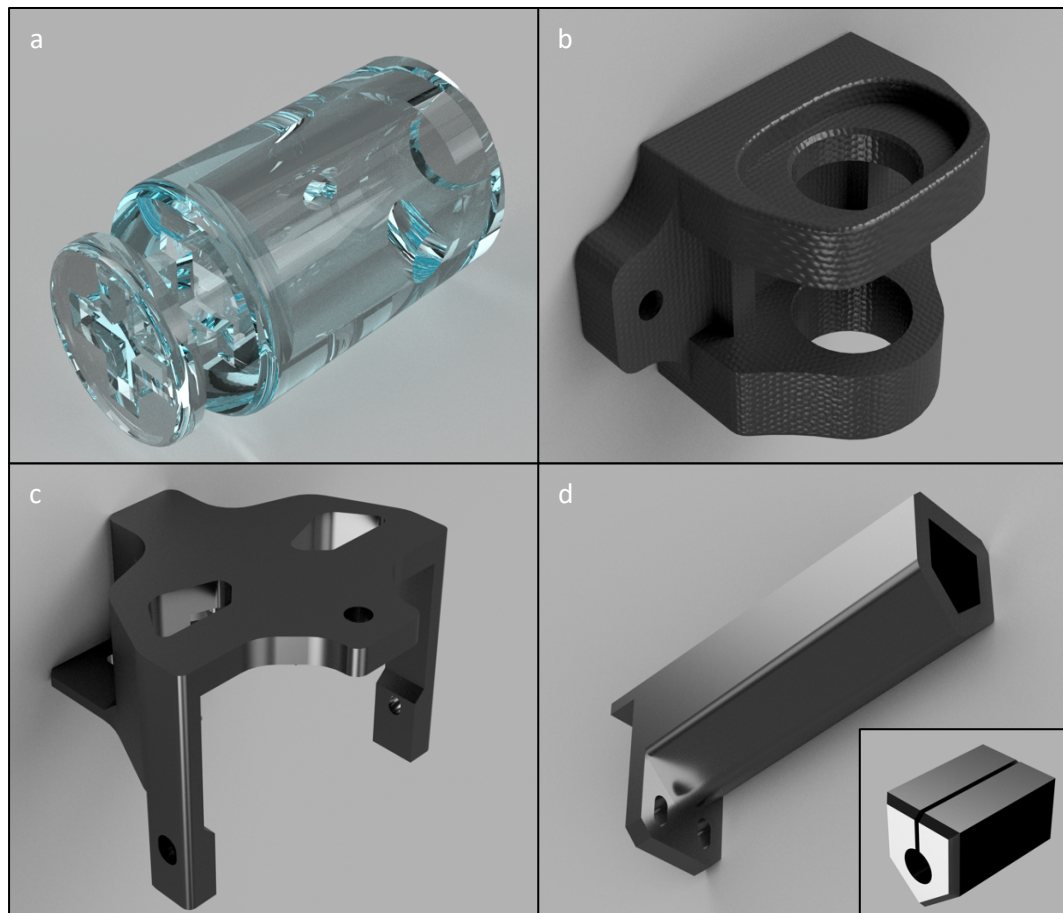


Figure 23: a) Piston cap made from natural PLA for sterilization requirement. b) Syringe cap but in rendered mode. c) 30 T5 Gear holding cap for optimum alignment and stabilization of the gears. d) Vertical tunnel guide for lead screw clamp to vertically move

Printing procedure of the parts

After the installation of the new 3D printer ender 5 pro and its calibration, Primavalue PLA was used for the construction of the bioprinting head. Packaging with the filament also includes instructions on the parameters the 3D printer has to be applied with so that the optimum quality print will be delivered. For the specific product, based on the instructions of the datasheet, 208 °C was applied to the printing head and 57 °C was applied to the bed surface of the 3D printer.

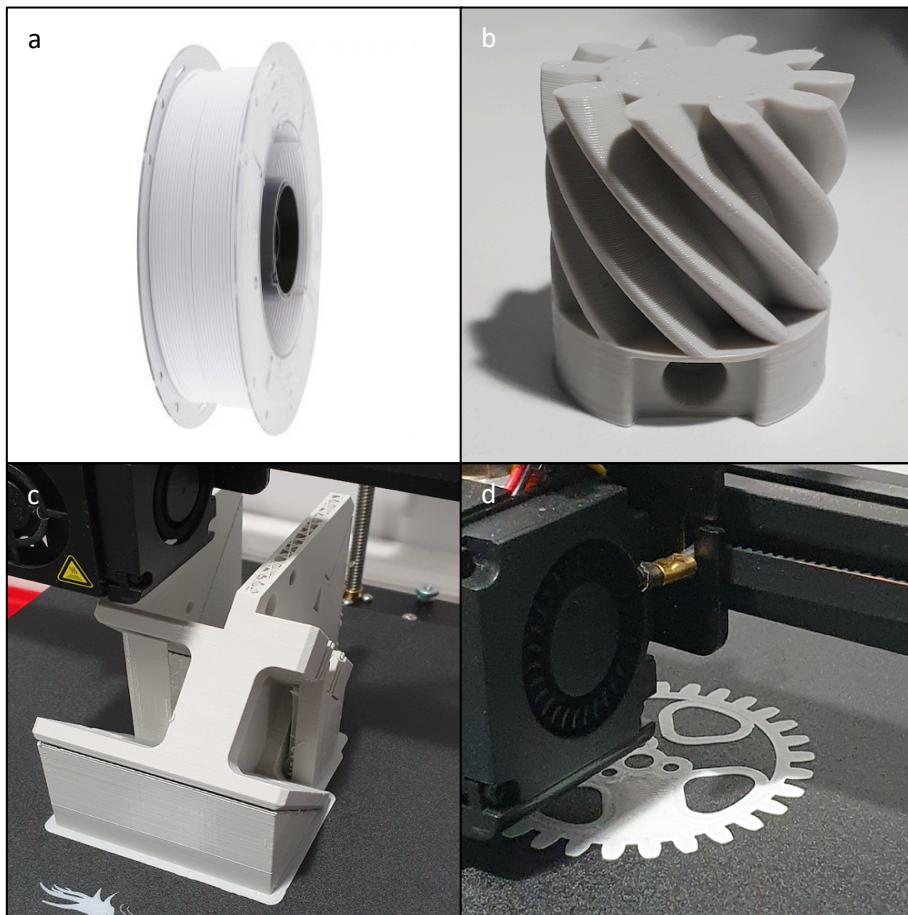


Figure 24: a) Filament PLA flex for the 3D printing procedure (Figure provided by grobotronics.gr). b) Optimum quality printed structure of the drive gear. c) Last few layers before the completion of the bioprinting head mount. d) 3D printing procedure of move gear

Based on their geometrical complexity, parameters had to be changed for the achievement of optimum printing quality of the parts. Printing speed, layer height, and generation of supports were the basic parametric commands that had to be modified in the slicer based on the part. For example, gears had to be printed at a 15 mm/s printing speed because of their sharp corners of the teeth and their small size, a layer height of 0.16 mm for better outer wall quality, and no support generation because of their well-placed angle on the bed surface.

On the other hand, the bioprinting head mount was printed at a 20 mm/s printing speed and a layer height of 0.20 mm for faster construction deliverance. Generation of supports was essential because of the complexity of the structure and its angle of print. The part was placed at a 45-degree angle to achieve longer printing surfaces caused by the diagonal printing procedure.

Final assembly of parts

After finishing and testing the printing quality and dimensions of the parts, a procedure of fastening was made to test the final structure of the assembly. Standardized M3, M5 screws, washers, and nuts were placed on the assembly model to attach and hold parts together. Nuts were permanently placed in pre-designed gaps of the printed parts via a thermal operation on their surface and by melting the printed part directly at a specific point, the attachment was achieved.

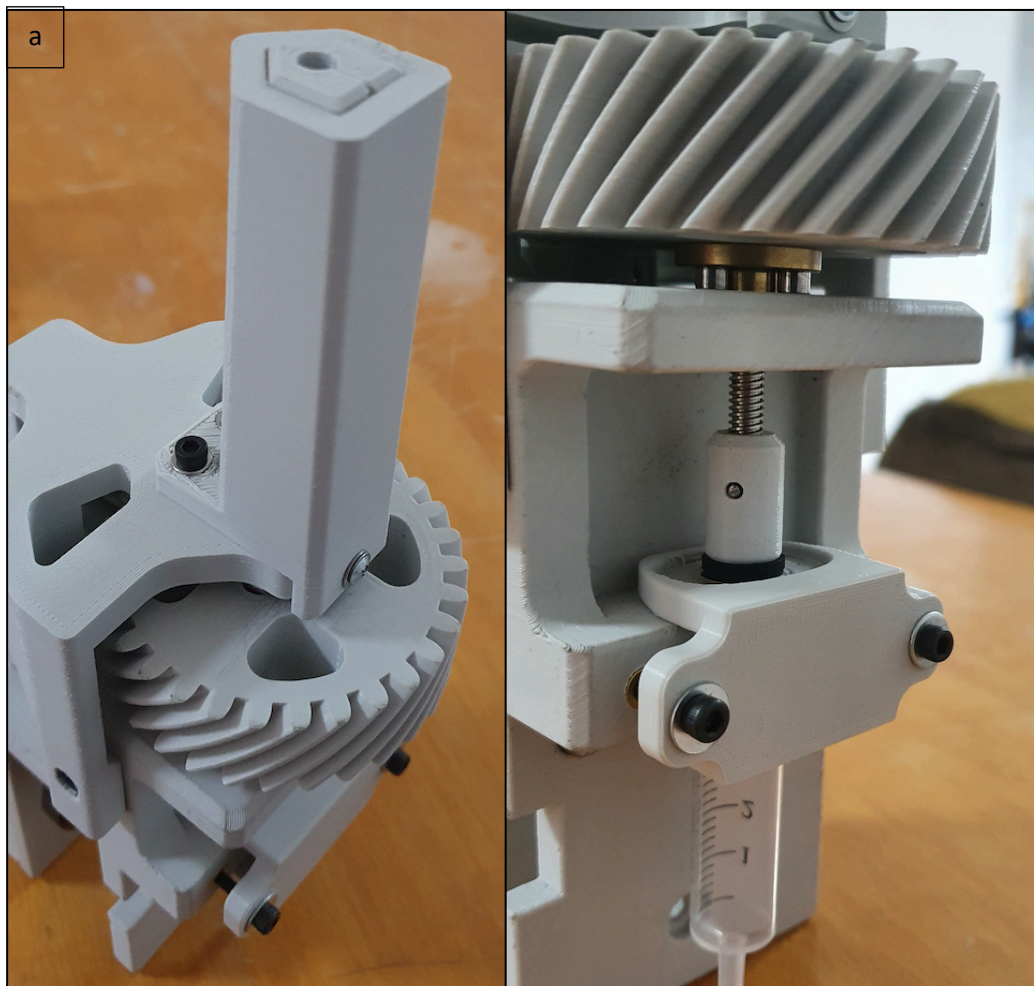


Figure 25: a) First physical assembly of the mechanism. b) Focused view for syringe attachment and calibration

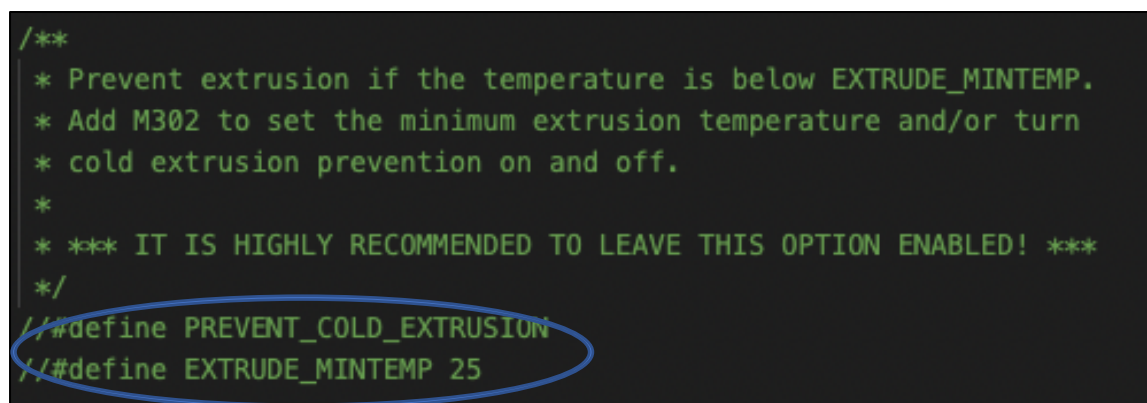
As soon as the assembly was completed, a manual rotational test was made to project and trial the alignment of the parts. The assembly seemed to be visibly aligned properly and while rotational tests were made, problematic friction or anomalies did not occur. The next step is the attachment of the mechanism on the standardized base of the 3D printer and the connection with electrical power for automation troubleshooting and trials.

Converting the mechanism into an automatism

In engineering, the term automation – mechatronic system comes from the cooperation of a mechanism with electrical power and a computing unit. Using a mechanism, human actions have to directly occur to deliver work or functionality. By converting the mechanism into an automation – mechatronic system, human action is now replaced by a computing unit that manipulates the mechanism via current and electronic signals. The 3D printer is considered a mechatronic system. By using the standardized methodology of the 3D printer, the extrusion stepper motor is the same. The only difference is that more steps need to be executed because of the difference in gear teeth, the ratio of the transmission, and the feed rate of the procedure. Operation on the cables of the 3D printer did not have to be applied, thus, modification in the firmware of the 3D printer was necessary.

The firmware is a construction of the code the 3D printer follows directly. It is written in programming languages such as C++ or Python but communicates with the printer in the binary language. In the firmware, protocols, safety-protection parameters, identification information, etc., are providing the printer information on what its purpose is. By living the firmware unmodified, the bioprinting head will not work properly. This is caused by the safety factors the firmware operates to the printer. For example, the safety net of this 3D printer does not allow extrusion of the filament in temperatures under 160 °C, warning -protecting the nozzle of the printing head from disfunction or even destruction.

In this case, while the bioprinter uses only mechanical pressure to extrude the fluid from the syringe's chamber, thermal power is not needed. If a trial of bioprinting is made, the safety net of the standardized bioprinter will not understand that there has been a modification and will shut down the printing procedure due to low temperature at the tip of the nozzle. Using the platform Visual Studio Code, modifications on the firmware and its safety parameters based on the thermal operation were re-written and a 'firmware.bin' file was exported and installed in the bioprinter.



```
/**
 * Prevent extrusion if the temperature is below EXTRUDE_MINTEMP.
 * Add M302 to set the minimum extrusion temperature and/or turn
 * cold extrusion prevention on and off.
 *
 * *** IT IS HIGHLY RECOMMENDED TO LEAVE THIS OPTION ENABLED! ***
 */
// #define PREVENT_COLD_EXTRUSION
// #define EXTRUDE_MINTEMP 25
```

Figure 26: Cropped view of firmware where using '/' the thermal safety factors are turned off

Preparation of the bioink

Now that the bioprinter is working properly, the preparation of the Cellulose Acetate – Acetone mixture could proceed. Mixtures of CA 10,20,30 wt% were prepared for viscosity behavior test into the syringe and smoothness of extrusion. From literature, results have already been delivered but in this research, a trial for parametric manipulation is sought. In 3 sealed containers, CA powder (Sigma-Aldrich) of 10,20, and 30 wt% and Acetone (Sigma-Aldrich) were used for 10 ml solutions. The solutions were mixed for 5 minutes with a magnetic stirrer and left for 5 hours to rest and become fluid. In these 5 hours of rest, the mixture also eliminates visible air bubbles from its original stirring. From experiments, temperature of 30-50°C made stirring easier as it temporarily lowered the viscosity of the solution.

Bioink mixtures 10 ml	
Cellulose Acetate Mn 30.000	Acetone 99.5%
1 gr	9 ml
2 gr	8 ml
3 gr	7 ml

Table: 3 Portions of mixtures for trials

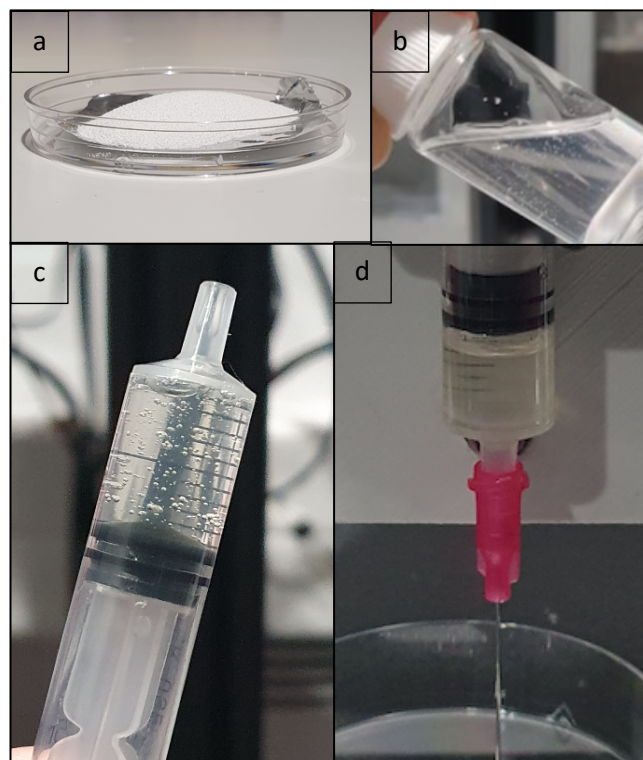


Figure 27: a) Visible powder portion of Cellulose Acetate. b) Solution in sealed container c) Bioink placed in the syringe for the first few seconds. d) Issue created on the top level of the bioink. Captured air creates a volume where pressure is not stable

First printing result

Given that the bioink was prepared, manual placement of the bioink into the syringe was performed and vertical movement of the piston sealed the container of the syringe. A standardized metal nozzle tip with gauge 22 and inner diameter 0.46 mm was placed at the tip of the syringe and calibration of height between the nozzle tip and bioprinter's bed was performed.

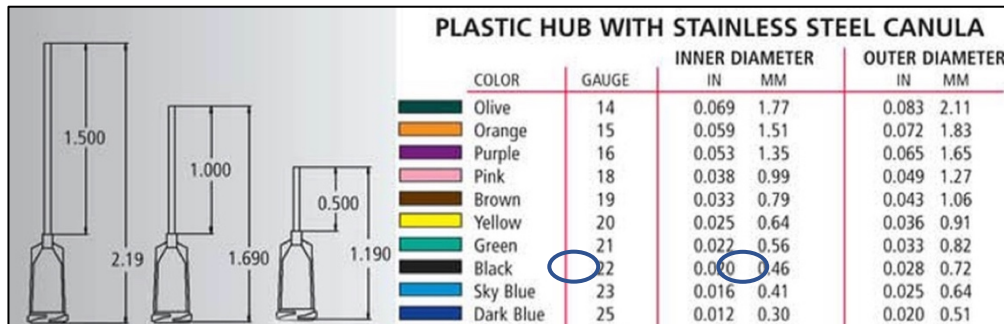


Figure 28: Figure of different categories of standardized syringes. Based on the color, gauge and inner diameter are given for the calculations

Based on the diameter of the nozzle tip, calculations were made in order to set the extrusion flow rate at an exact number (table 4). Extrusion flow rate is a complicated parametric procedure with calculations, using several parameters to achieve the best condition of printing speed and extrusion flow rate for the optimum result. From the parametric table 3 presented above, the critical number was the printed length, which would specify the printing parameters set in the Gcode, to produce the desired structure. Each 1 mm of printed fluid requires the piston to move 0.00127 mm into the syringe.

PRINTING CALCULATIONS (mm)	
Diameter (syringe)	14,57
Diameter (nozzle)	0,46
Area (syringe)	166,6436465
Area (nozzle)	0,166106
eSteps / mm	4800
w (printed width)	0,46
h (printed height)	0,46
Ls (syringe length) mm	0,001269775
Lp (printed length) mm	1
eSteps for Printed length	6,094921837

Table: 4 Printing calculations for optimization of Gcode

$$L_S = \frac{w \cdot h \cdot L_p}{A}$$

From the results presented in table 3, the parameters were set for the first bioprinting test. While experiencing a few issues with the pre-installed material and texture of bed from the ender 5 pro printer, aluminum leaf showed great attachment of extruded material while printing, and also dis-attachment without hurting the scaffold was achieved. By using the bioink with 30 wt% Cellulose Acetate, an 8-layer scaffold was delivered in 10x10x1.2mm size.

Preliminary Cell Study on CA scaffolds

For all cell cultures at this study, mouse Mesenchymal Stem Cells (MSC) C57BL/6 were used. MSCs are multipotent stem cells that can differentiate into a variety of cell types including osteocytes, adipocytes, and chondrocytes. They are capable of proliferating and generating a local immunosuppressive microenvironment, thus contributing to their wide application potentials in tissue engineering, cell therapy, and gene therapy. MSCs have a strong capacity for self-renewal while maintaining their multipotency.

The cells were grown in cell culture flasks using Dulbecco's modified Eagle's medium (DMEM) – Low glucose (1000mgr/L glucose) supplemented with 10% fetal bovine serum (FBS) and 1% penicillin/streptomycin solution (PS) at 37°C in a 5% CO₂ incubator, with medium renewal every 3-4 days. All cells used for the experiments were in a passage, ranging from 7-10. CA scaffolds were UV sterilized and transferred into sterile wells of 24-well plates. 100000 cells/ml in culture medium were seeded on the samples and were cultured for 1 and 3 days . Tissue culture plastic (TCP) coverslips were the control samples (reference material) in all the experiments.

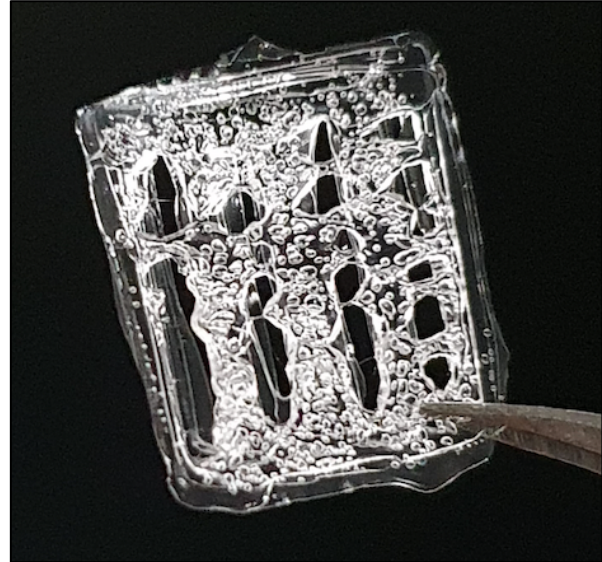


Figure 29: First bio printed scaffold. Failed print caused of trapped air and flow rate miscalculation

Scanning electron microscopy (SEM): preparation of the biological samples - dehydration procedure

The cells growing on the CA scaffolds and TCP samples were analyzed by the SEM microscope (JEOL). After each time point, the cells were fixed following a specific fixation protocol. The medium was removed from samples, and they were washed twice with 0,1M Sodium Cacodylate Buffer (SCB) (pH = 7,4) for 5 min in 4oC. Then they were fixed with 2,5% glutaraldehyde (GDA) / 2,5% paraformaldehyde (PFA) in SCB fixative buffer for 30 min at 4oC. The samples were then washed twice (for 5 min each time) with 0,1M SCB at 4oC. The samples at dehydration phase were washed in graded series of 30%, 50%, 70%, 90%, and 100% EtOH for 10 min each at 4oC. Then, the samples were transferred into a chemical hood and immersed in hexamethyldisilazane HDMS)/ EtOH (50:50) solution for 30 min and 20 min, then, in 100% HDMS for 20 min twice at 4oC. As a final step, HDMS was removed, and samples left to dry completely overnight at the chemical hood. Prior to electron microscopy examination, the samples were sputter-coated with a 15nm film of Au (BAL-TEC SCD 050).

Chapter 5: Discussion and analysis of findings

Optimization process for the successful Cellulose Acetate printing

From the result of figure 30, it is visible that one issue that created interference with the deliverance of the scaffold was the air trapped in the fluid. While bioprinting it was noticed that a visible amount of air was trapped in the chamber of the syringe creating anomalies while extruding. It was noticeable that extrusion was happening in a higher feed flow than the one that had been set. That was a result of entrapped air pushed by the piston into the fluid creating air bubbles while extruding. By research on how to remove air on standardized syringes, a technician applied force on the outer plastic chamber of the syringe, deforming it into an ellipse, and letting the entrapped air leave the chamber.

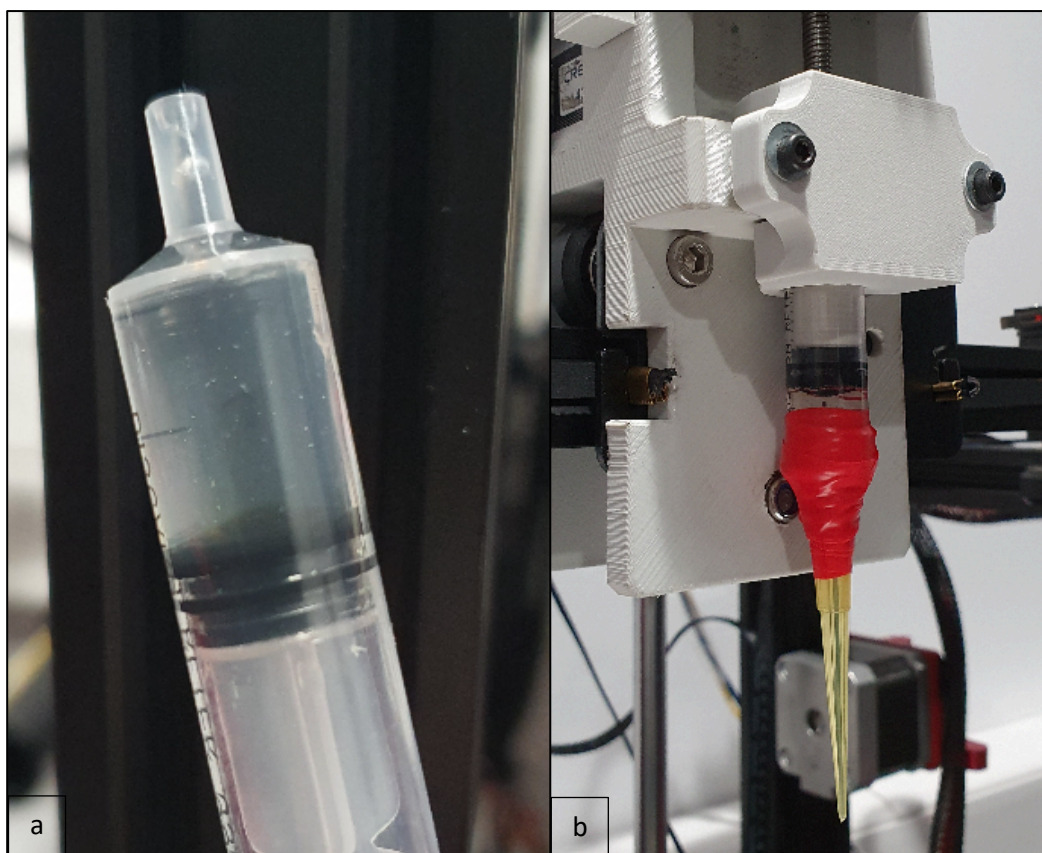


Figure 30: a) By inverting the syringe, trapped air ventilates and after 5 minutes rest, air bubbles disappear. b) Attaching a conical 22-gauge tip for tests

Now that entrapped air left the chamber, a re-design of the scaffold was delivered and another trial of bioprinting was made. Printing speed was set to 3,5, and 10 mm/s to check the printability behavior of the material. Manipulating the printing speed, the solidification of the bioink was affected by the evaporation of the Acetone, when it came in contact with the environment. The slower the printing speed, the faster the solidification when printing layer-by-layer. Thus, an average condition had to be secured because while printing, each layer needed to be attached with the other, meaning that while printing the second layer, the first layer had to be in a semi-solid condition in order to be attached with the above one. For that specific reason, different printing conditions were tested for the best possible outcome.

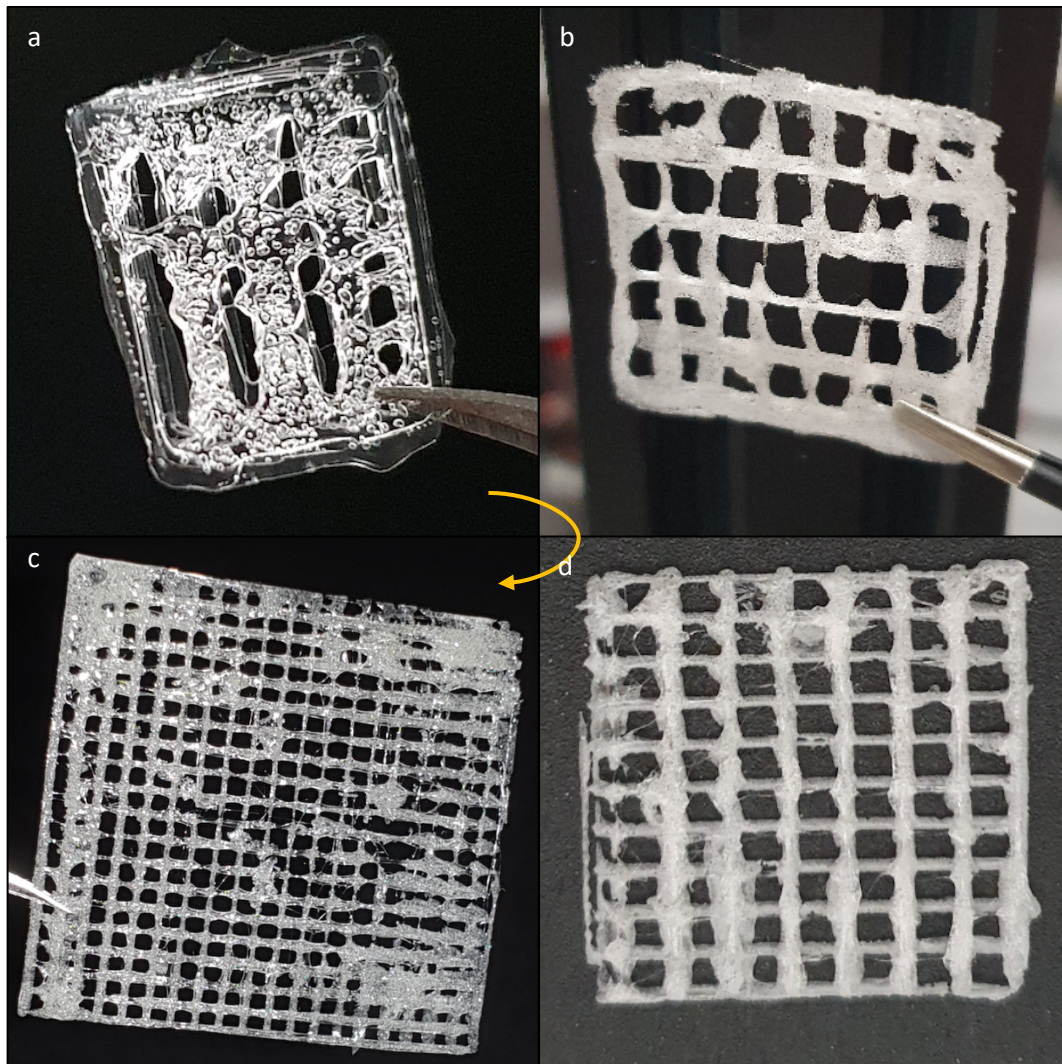


Figure 31: a) Bioprinting test 1 (failed, creation of trapped air bubbles, flow rate miscalculation, no size accuracy. b) Bioprinting test 2 (formed structure but flow rate was miscalculated again). C) Bioprinting test 3 (achieved printing dimensions, accuracy in creating rectangles, flow rate optimization and surface of bed affected the printability) multilayer structure of 16 layers. d) Bioprinting test 4 (solid form, requirement of further flow rate optimization, printing speed optimization and calibration of bed)

Comparing the results with literature's

Even though further modification had to be done for the bioprinter to deliver the optimum geometries, by changing the parameters on the above-presented samples it is clear that the rectangles constructing this thesis' scaffold are sharper and strict to their edges compared to the samples presented in the literature. Thus, that is a result only for 700 μm rod-distance. While making trials on printability, new parameters will come up to the surface, providing greater resolution each time. (Hanxiao Huang, 2019)

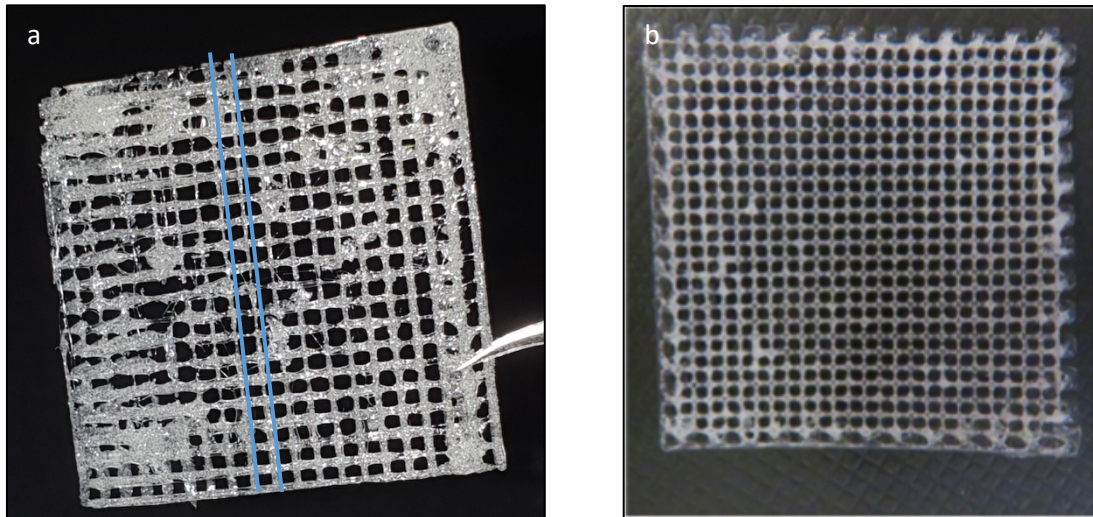


Figure 32: a) Based on bioprinting test 4, rod distancing was calculated 700 μm b) Bioprinting test from literature above mentioned, 1000 μm rod-distancing

Further optimization in Gcode was tested in order to deliver greater results, not only in 1- or 2-layer scaffolds but 8- and 10-layer scaffolds. The redeveloped Gcode avoids commands which in fig.53 extruded higher portion of material than expected, creating material pools ruining the scaffold's symmetrical pattern. Rewritten commands now order the bioprinter to print only in one way path, avoiding travelling on surfaces that already have material while there is no extrusion. Because of the form of the fluid, material does not solidifies instantly offering the bioprinter's nozzle to pass through it and reform it or even change its geometry. With the one-way path Gcode, the bioprinting head passes only once from the extrusion path and then rises in order to travel without extrusion.

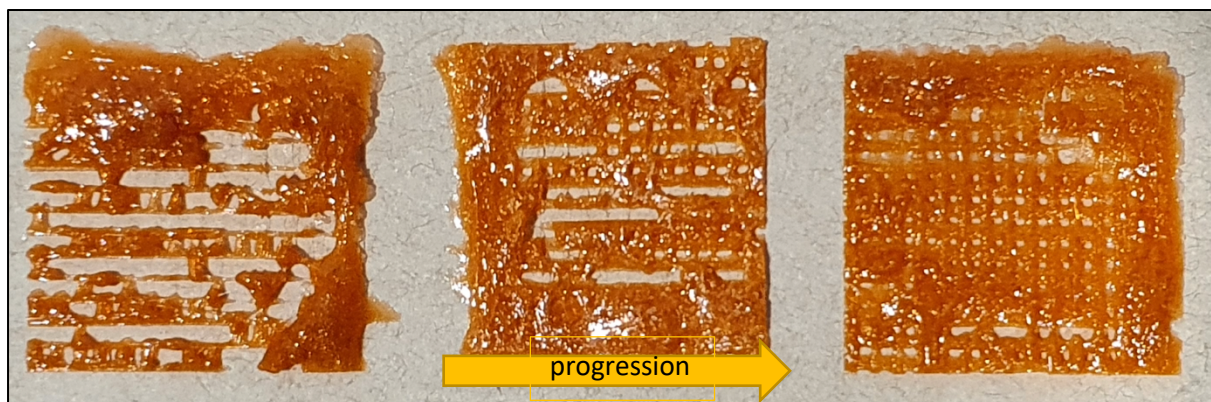


Figure 33: Modification in Gcode in order to deliver optimized results from mixture of Cellulose Acetate 25wt%, mixed with alizarin red powder for observation while extruding the lines

The redevelopment of Gcode offered greater results than the modification of the recipe because it offered a variety of parameters to change in order to deliver an acceptable resolution, instead of the limited modification of viscosity the recipe offered. By changing the travel speed to 100mm/s, the printing speed to 5mm/s and the rise of the Z axis every time a line was printed, the printability thrived.

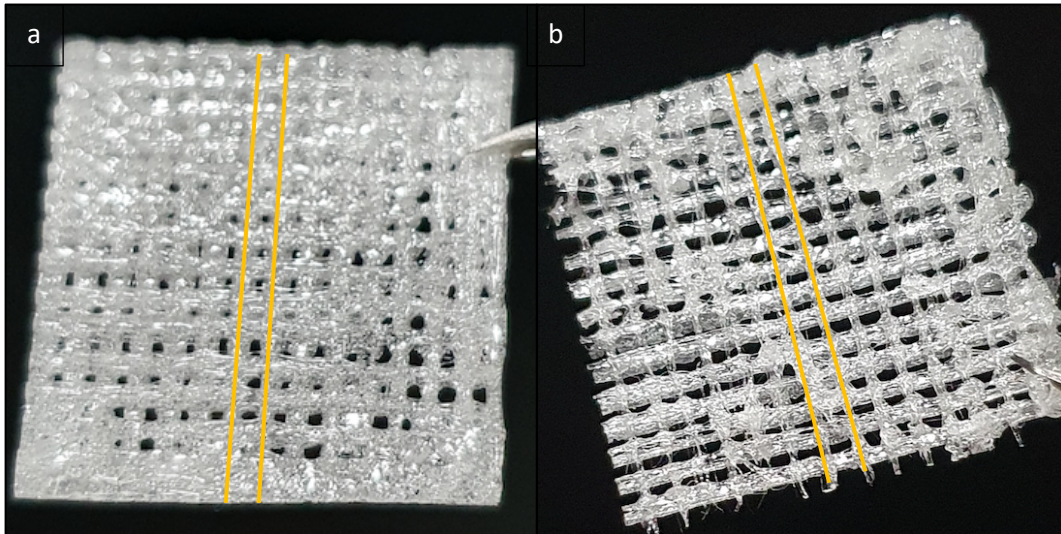


Figure 34: a) Cellulose Acetate 25wt% - 10 layer scaffold with rod-to-rod resolution 400 μm b) Cellulose Acetate 40wt% - 10-layer scaffold with rod-to-rod resolution 300 μm (woodpile architecture)

Further investigation in the architectural structure of the scaffolds was achieved via the use of Scanning electron microscopy (SEM) system, which produces images of selected samples by scanning their surface with the use of a focused beam of electrons. After the production of the scaffolds, a process called sputter coating creates a surface of gold nanoparticles which are highly conductive, helping the SEM imaging to produce better quality images.

This imaging process will provide information of the printing quality, the symmetry of the scaffolds that are being produced, but also the compatibility of the fabricated environment for the cells to proliferate and differentiate.

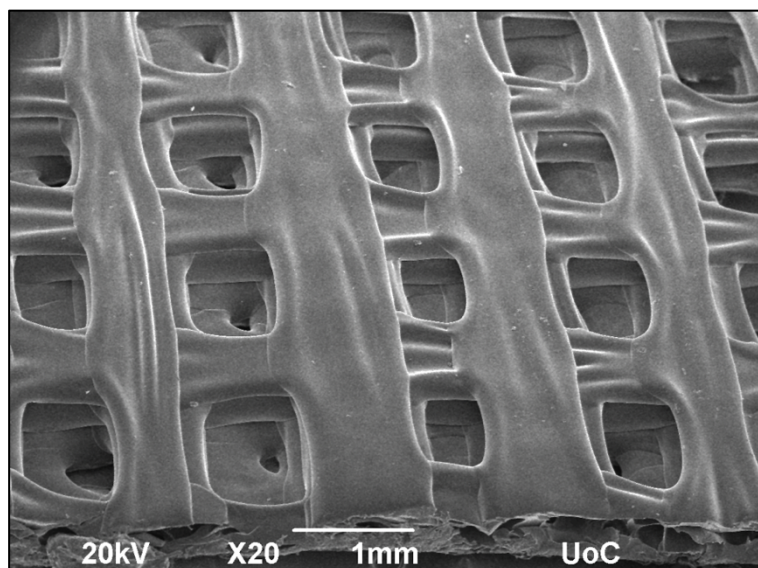


Figure 35: Cellulose Acetate 25wt% - 10-layer scaffold with rod-to-rod resolution 400 μm . Provided by University of Crete via SEM imaging

Biocompatibility – Toxicity tests

From the literature review (Courtenay, Sharma, & Scott, 2018), one of the most promising polysaccharide-based biomaterials is Cellulose. Much attention has been given to Cellulose because of its ability to offer properties for scaffolding structures. Mentioning its biocompatibility, Cellulose offers the ability to get modified in order to achieve parametric mechanical properties, setting it as a promising biomaterial for the future of tissue engineering. Offering these biocompatible properties, Cellulose is a material that could be used in a bioink composition for printing a 4D scaffold with different porous sizes. The preliminary cytocompatibility study of the 4D CA scaffolds was performed for 1 and 3 days. There were TCP disks as controls showing the cells viability and morphology on 2D substrates. MSCs proliferated and attached well on the 4D CA surface, and in between the layers for

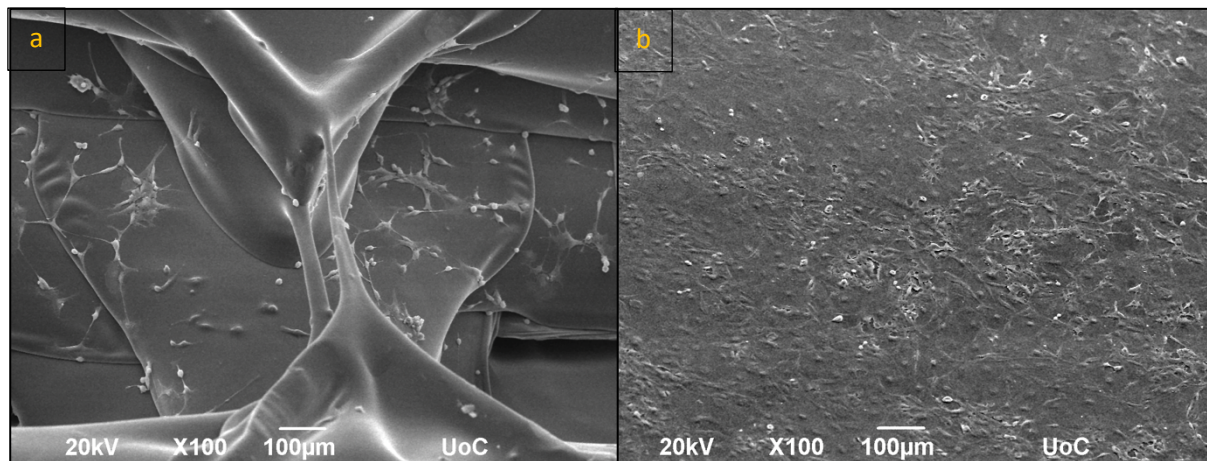


Figure 36: Tilted view SEM images of a) CA 25wt% Scaffold b) Tissue culture plastic) with MSCs for 1 day (cell concentration 100.000 cells/ml or sample).

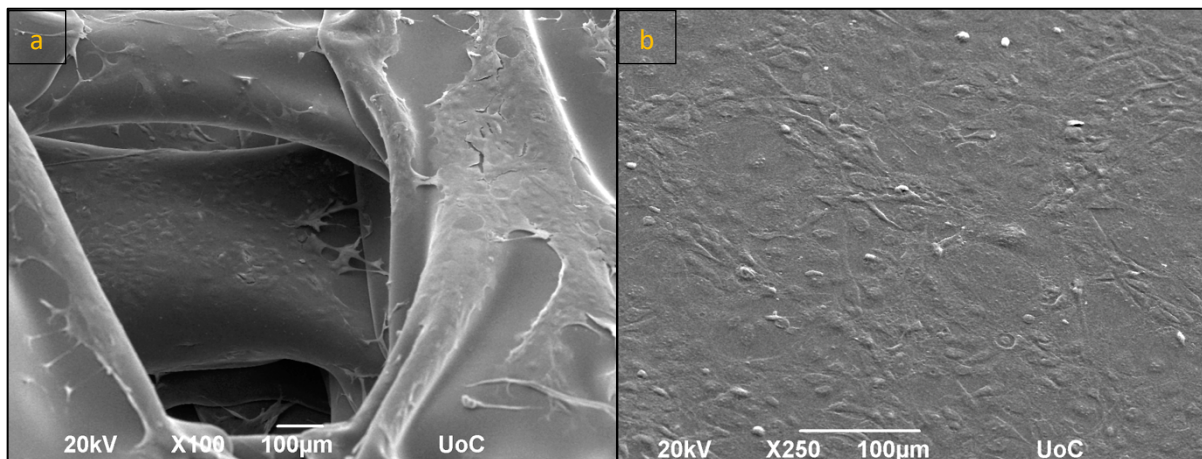


Figure 37: Tilted view SEM images of a) CA 25wt% Scaffold b) Tissue culture plastic) with MSCs for 3 day (cell concentration 100.000 cells/ml or sample).

the 1 and 3 days of culture. Specifically, at 1 day the cells appeared to be more adhered on the layers below the top layer. There were MSCs with circular and with a branch shaped morphology indicating good adhesion and cell communication. At 3 days, the cells exhibited a flattened morphology demonstrating great adhesion and proliferation similar to the TCP disk. All the layers were covered with cells even the top layer.

The main observation from the SEM images of Fig. 35-36 was that the cells attached well and proliferated (for both time points) on the CA scaffolds, and in between layers mainly at 3 days.

Also, if a sterilized environment can be achieved, trials for direct cell extrusion can be operated..

Comparing structure architecture with efficiency

Proceeding with further observation of the architecture of the scaffolds in figure 38, it is visible that the top surface of the scaffold in figure 38a offers a uniform smooth surface. Contrariwise, in figure 38b, the texture of the bottom layer seems to be rough and textured, while uniformity does not exist. The visible roughness was occurred during the detachment of the scaffold from the bed.

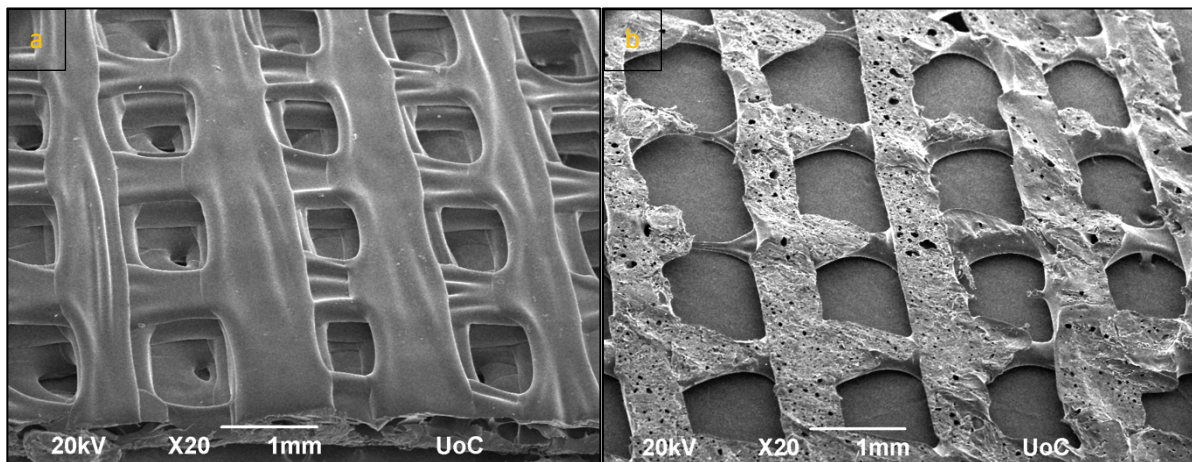


Figure 36: Difference in surface texture and structure of scaffolds. a) Top view placement b) Inverted scaffold view (both scaffolds where made from a CA 25wt% solution)

The different placement of the surfaces presented in figure 38,39 was a random result, which was observed in SEM imaging while samples were placed on plates normally and inverted by lack of visibility of the surfaces. Though, this random misplacement showed the difference in both the surfaces and the cells-cultured on them.

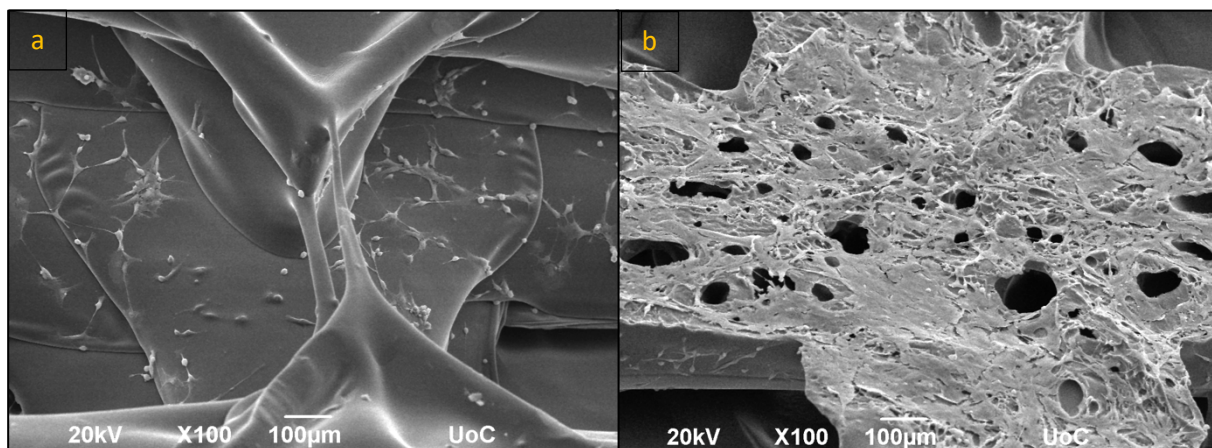


Figure 37: Morphology of the surfaces seems to not affect the cell-proliferation in day 1 in a visible level (both scaffolds where made from a CA 25wt% solution)

How uniformity is affected

After optimization of the parameters was at a final stage, the production of samples came to a troubleshooting conclusion. While the nozzle deposits fluid on the bed surface, Acetone evaporates from the solution rapidly, creating a semi-solid mass on the nozzle tip. That semi-solid mass drifts the deposited material on the printing path while creating irregularities on the surface of the printed scaffold. In order to avoid this irregularity, a user-caring (user's hand removes material with a cleaning tool) has to be applied, detaching the semi-solid material from the nozzle while printing progresses. Presented in figure 40a, user-caring was applied at a maximum level, in contrast with figure 40b in which no user-caring was applied.

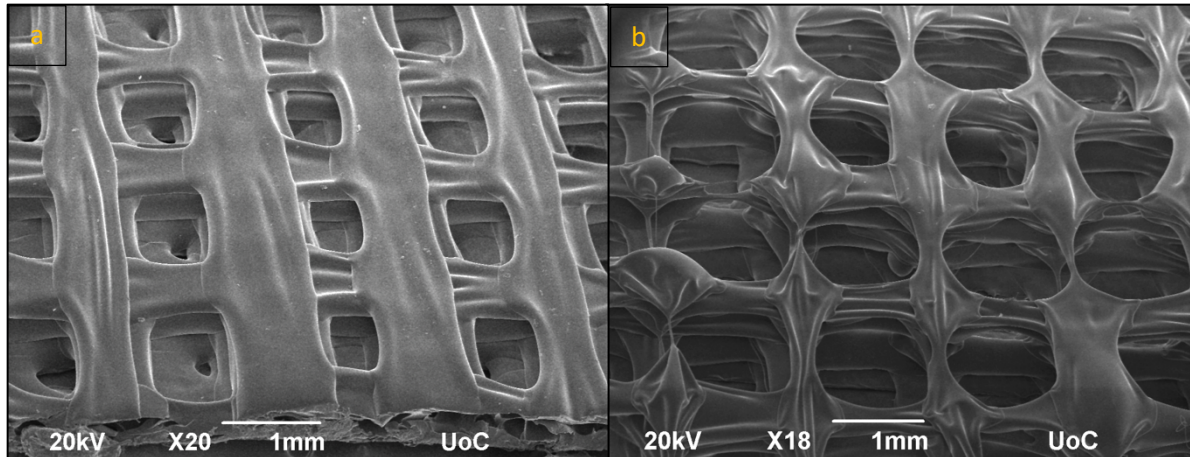


Figure 38: a) Maximum user-caring CA 25 wt% 10-layer scaffold presenting a uniform architecture. b) No user-caring CA 25 wt% 10-layer scaffold presenting irregular architecture

In Figure 41, Further investigation has to be occurred. Though, both scaffolds (fig40a-b) showed good potential in cell spreading through the layers of the scaffolds (from the bottom to the top layers). From the tilted view of SEM imaging, both 9th and 10th layers (bottom layer = 1) of the scaffold showed similar allocation of the cells on the surfaces.

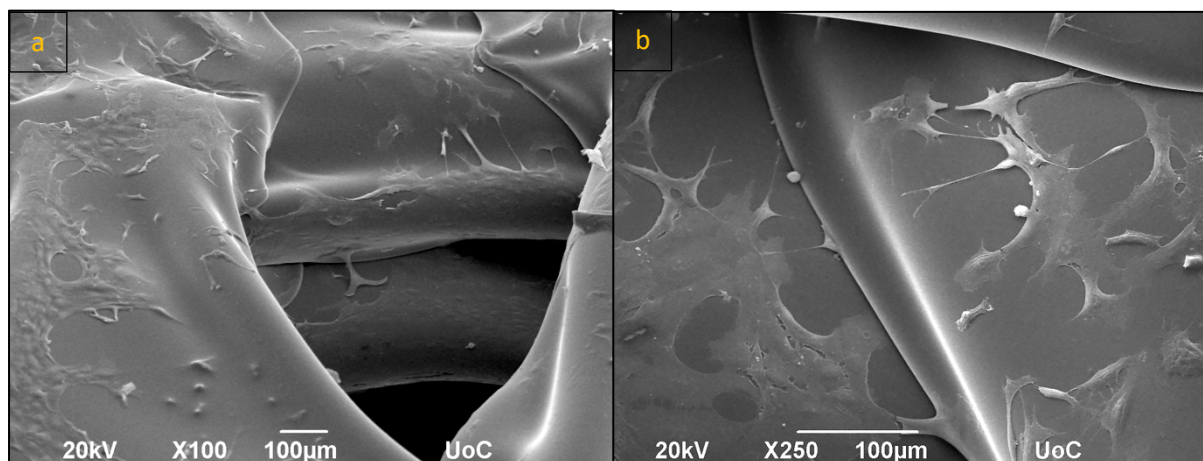


Figure 39: Observation of cellular responses such as adhesion and proliferation through the a) user-caring and the b) no user-caring 3D scaffold.

Chapter 6: Conclusion and recommendations

3D – 4D bioprinting is continuously showing its importance in the future of regenerative medicine and tissue engineering. It is a promising technique, recently introduced, which evolves day by day constructing a library of knowledge and results, solving problems in the most novel ways possible. Since the science behind regenerative medicine evolves, more funds and attention from scientists and companies will be given in the next years. The purpose of this thesis research is the presentation of a super-low-cost parametric conversion of a 3D printer to a 3D-4D bioprinter, providing a nominal design for the user to modify based on the 3D printer provided, a parametric board of calculations explained and solved based on the requirements of the technology used.

The supply proposal of low-cost biomaterials, the troubleshooting through the process, and the promising future development of this project could offer an interesting proposal for scientists in biology, material science, medical, and engineering field to start developing their scaffolding samples, culturing, and trying to find a way of guided proliferation and differentiation of cells based on the geometrical structure of the scaffold.

It is known that innovation and greater development arrive from the higher number of scientists researching and combining knowledge to find a solution. This custom super-low-cost 4D bioprinter costs about 60 euros making it a great proposal for future research and development. Instructions on how to use it are offered through this thesis research, providing the user a plug-n-play experience. Another proposal for future research and development is the combination of cellulose with gelatin or alginate mixtures to create gelatinous 4D scaffolds (figure 42), offering different mechanical properties and structures for cells growth and proliferation.

To conclude, additive manufacturing and more specifically 4D bioprinting tend to be the most successful trending development in tissue engineering, promising regeneration and self-healing for tissue, organoid, and organs like no other section of medicine could offer until now.

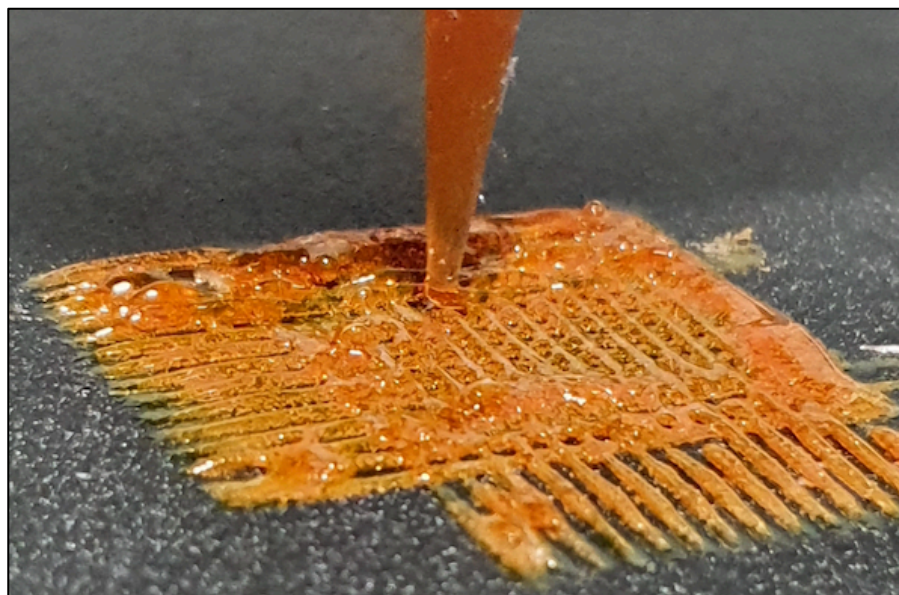


Figure 40: Bioprinting process of a Cellulose Acetate – Gelatine 10-layer scaffold.

References

- Ankita Jaisingh Sheoran, H. K. (2019). Fused Deposition modeling process parameters optimization and effect on mechanical properties and part quality: Review and reflection on present research. *materialstoday*, 1659-1672.
- Asadian, M. &. (2020). Fabrication and Plasma Modification of Nanofibrous Tissue Engineering Scaffolds. *Nanomaterials*.
- Askari, M., Afzali Naniz, M., Kouhi, M., Saberi, A., Zolfagharian, A., & Bodaghi, M. (2020). Recent progress in extrusion 3D bioprinting of hydrogel biomaterials for tissue regeneration: a comprehensive review with a focus on advanced fabrication techniques. *Biomaterials Science*.
- Bowen, J. (2020, February). *Bioprinting: Building the Future of Medicine, Layer by Layer*. Retrieved from Nexight group: <https://www.nexightgroup.com/bioprinting-building-the-future-of-medicine-layer-by-layer/>
- C. Norotte, F. M. (2009). Scaffold-free vascular tissue engineering using bioprinting. *Biomaterials*.
- Cho Ki-Hyun, P. F. (2020). Mixed Reality and 3D Printed Models for Planning and Execution of Face Transplantation . *Annals of Surgery*, Volume 274, Number 6.
- Close P. Gouma, R. X. (2012). Nano-hydroxyapatite-Cellulose acetate composites for growing of bone cells. *Mater. Sci. Eng.*
- Courtenay, J., Sharma, R., & Scott, J. (2018). Recent Advances in Modified Cellulose for Tissue Culture Applications. *Molecules*.
- Daar, A. S., & Greenwood, H. L. (2007). A proposed fedinition of regenerative medicine. *Journal of Tissue Engineering and Regenerative Medicine*, 179-184.
- Fa-Ming Chen, X. L. (2015). Advancing biomaterials of human origin for tissue engineering. *Elsevier*.
- Gi Hoon Yang, M. Y. (2019). 4D Bioprinting: Technological Advances in Biofabrication. *Macromolecular Bioscience*.
- Hanxiao Huang, D. D. (2019). 3-D printed porous cellulose acetate tissue scaffolds for additive T manufacturing. *Additive manufacturing (Elsevier)*.
- Hanxiao Huang, D. D. (2020). 3-D printed porous cellulose acetate tissue scaffolds for additive manufacturing. *Additive Manufacturing*.
- Kang, H. L. (2016). A 3D bioprinting system to produce human-scale tissue constructs with structural integrity. *Nat Biotechnol*, 312–319.
- Konstantinos Ioannidis, R. I. (2020). A Custom Ultra-Low-Cost 3D Bioprinter Supports Cell Growth and Differentiation . *Frontiers*.
- M.N. Nosar, M. S. (2016). Characterization of wet-electrospun cellulose acetate based 3-dimensional scaffolds for skin tissue engineering applications: influence of cellulose acetate concentration. *Cellulose*.

- Ma, P. X. (2004). Scaffolds for tissue fabrication. *materialstoday*, 30-40.
- Morouço, P., Azimi, B., Milazzo, M., Mokhtari, F., Fernandes, C., Reis, D., & Danti, S. (2020). Four-Dimensional (Bio-)printing: A Review on Stimuli-Responsive Mechanisms and Their Biomedical Suitability. *Applied Science*.
- N. Noor, A. S. (2019). 3D printing of personalized thick and perfusable cardiac patches and hearts. *Adv Sci*.
- Prafulla K. Chandra, S. S. (2020). Tissue engineering: current status and future perspectives.
- Radhakrishnan, S. N. (2020). Fabrication of 3D printed antimicrobial polycaprolactone scaffolds for tissue engineering applications. *Materials Science and Engineering*.
- Rose, A. S., Webster, C. E., Harrysson, O. L., Formeister, E. J., Rawal, R. B., & Iseli, C. E. (2015). Pre-operative simulation of pediatric mastoid surgery with 3D-printed temporal bone models. *International Journal of Pediatric Otorhinolaryngology*.
- T.J. Hinton, Q. J. (2015). Three-dimensional printing of complex biological structures by freeform reversible embedding of suspended hydrogels. *Sci Adv*.
- W. Sun, B. S. (2005). Bio-CAD modeling and its applications in computer-aided tissue engineering . *Computer-Aided Design*, 1097-1114.
- Yaewon Park, X. C. (2020). Water-responsive materials for sustainable energy applications . *Journal of Materials Chemistry A*.
- Zeming Gu, J. F. (2020). Development of 3D bioprinting: From printing methods to biomedical applications . *Asian Journal of Pharmaceutical Sciences*, 529-557.
- Chen, X., Han, S., Wu, W., Wu, Z., Yuan, Y., Wu, J., Liu, C., *Harnessing 4D Printing Bioscaffolds for Advanced Orthopedics. Small* 2022, 2106824.